(4)

AD-A271 610

Technical Document 2569
October 1993

A New Matrix Formulation of Classical Electrodynamics

Part III. Wave Propagation
Through A Multilayer Dielectric
Medium With Planar Boundaries

R. P. Bocker

DTIC
ELECTE
OCT 28 1993
S B D

93-25875

NRaD

93 10 25 0

A New Matrix Formulation of Classical Electrodynamics

Part III. Wave Propagation Through A Multilayer Dielectric Medium With Planar Boundaries

R. P. Bocker

**NAVAL COMMAND, CONTROL AND
OCEAN SURVEILLANCE CENTER
RDT&E DIVISION
San Diego, California 92152–5001**

K. E. EVANS, CAPT, USN
Commanding Officer

R. T. SHEARER
Executive Director

ADMINISTRATIVE INFORMATION

ACKNOWLEDGMENTS

MA

ABSTRACT

A new approach for solving electromagnetic wave propagation problems is currently being developed at the Naval Command, Control and Ocean Surveillance Center (NCCOSC), RDT&E Division (NRaD). This new approach is based upon an 8 by 8 matrix representation of the Maxwell field equations. In addition, a computer software package based on this matrix representation of electromagnetic theory is also being written and tested at NRaD to handle a variety of scenarios involving electromagnetic wave propagation through matter. This software package is referred to as the MATURE Program. MATURE is the acronym for Matrix Approach To Understanding Relativistic Electrodynamics. The MATURE Program is written in MATLAB code for use on a Sun 4 SPARCstation 2 workstation. Under Independent Research (IR) FY 92 funding, this matrix approach was successfully employed in solving problems dealing with electromagnetic wave propagation through dielectric, crystalline, linear electro-optic, and magneto-optic materials of infinite extent. Under the Office of Naval Research (ONR) FY 93 funding, this matrix formulation was extended to handle problems involving wave propagation through multilayer dielectric media with planar boundaries. Presented in this technical document is the underlying theory of this matrix approach. Several numerical examples, based on the use of the MATURE Program, are also included to illustrate the use of the matrix approach in solving electromagnetic wave propagation problems.

i

CONTENTS

FIGURES

1.0 INTRODUCTION

In Part I of this series (Bocker & Frieden, 1992), a new matrix formulation of classical electromagnetic theory for vacuum is presented. The basis of this formulation is a skew-Hermitian space-time 8 by 8 differential matrix operator. There it was shown that the vector form of the Maxwell field equations for vacuum can be cast into a compact matrix form. From the matrix form of the Maxwell field equations, other fundamental results of electromagnetic theory are easily derived with use of the simple matrix multiply operation: (1) the electromagnetic wave and charge continuity equations; (2) the Lorentz- and Coulomb-gauge definitions of the electromagnetic potentials; (3) the wave equations for the potentials; and (4) Poynting's theorem on energy conservation. Taking the four-dimensional Fourier transform of the matrix form of Maxwell's equations leads to: (5) a Fourier representation of the Maxwell field equations; (6) their inversion, for the fields directly in terms of the sources in Fourier-space; and (7) corresponding inversion formulae in direct-space through the use of the convolution theorem. In Part II of this series (Bocker, 1992), the 8 by 8 electromagnetic matrix formulation for vacuum was extended to include the presence of matter. Emphasis was placed on electromagnetic wave propagation through linear, homogeneous, and anisotropic optical materials of infinite extent without boundaries. The matrix form of the Maxwell field equations was cast into an 8 by 8 matrix eigenvalue representation. In this technical document, we present the underlying theory for solving electromagnetic wave propagation problems involving multilayer dielectric materials with parallel planar boundaries. The matrix representation of the Maxwell field equations plays a central role in this investigation as well. As will be shown, boundary conditions are automatically taken into account by partitioning both the electromagnetic wavefunctions and the dielectric, permeability, and conductivity matrices of the dielectric medium using Heaviside unit step functions.

Because of the power of matrix operations, many of the fundamental relationships and results in electromagnetic wave propagation theory are easily derived without the need for the usual plethora of vector calculus identities that have become the standard in these derivations. Instead, mathematical operations involving matrix multiplication, matrix inversion, and eigensolutions of matrices can be employed. Available off-the-shelf computer software packages, like MATLAB and MATHEMATICA, are well suited for these matrix operations. A computer software package entitled MATURE is currently being written and tested at NRaD to handle a variety of scenarios involving electromagnetic wave propagation through matter. MATURE is the acronym for Matrix Approach To Understanding Relativistic Electrodynamics. The MATURE program is being written in MATLAB code for use on a Sun 4 SPARCstation 2 workstation.

1

2.0 THEORY

In this section, we will derive the equations for predicting the reflection and transmission characteristics of a multilayer dielectric medium with planar boundaries illuminated by a monochromatic electromagnetic plane-wave. We will begin with the vector form of the Maxwell field equations for matter. The vector form of the Maxwell field equations will then be cast into the compact matrix form described in Parts I and II of this series. The matrix form will then be specialized to dielectric materials. Next, the dielectric medium will be partitioned into a multilayer medium with planar boundaries using Heaviside unit step functions. As will be shown, the electromagnetic boundary conditions at each of the planar interfaces will be automatically taken into account using this approach. Then, monochromatic electromagnetic plane-wave solutions will be considered. This will lead to system operator description of wave propagation through the multilayer medium. The operator description will then be used to calculate the reflection and transmission characteristics of the multilayer medium for arbitrarily chosen wavelengths, angles of incidence, and polarization states of the incident electromagnetic radiation.

2.1 THE MAXWELL FIELD EQUATIONS

The fundamental equations of classical electromagnetic phenomena, namely the Maxwell field equations, serve as our starting point. In the Gaussian system of units, the four Maxwell field equations in vector form are given by the following (Jackson, 1962):

Ampere-Maxwell law

$$\nabla \times H(r, t) = \frac{1}{c}\frac{\partial}{\partial t}D(r, t) + \frac{4\pi}{c}J^e(r, t) \tag{1}$$

Gauss' law for electricity

$$\nabla \bullet D(r, t) = 4\pi\rho^e(r, t) \tag{2}$$

Faraday's law of induction

$$\nabla \times E(r, t) = -\frac{1}{c}\frac{\partial}{\partial t}B(r, t) - \frac{4\pi}{c}J^m(r, t) \tag{3}$$

Gauss' law for magnetism

$$\nabla \bullet B(r, t) = 4\pi\rho^m(r, t). \tag{4}$$

The physical quantities appearing in the Maxwell field equations are: $E(r, t)$ the electric field; $D(r, t)$ the electric displacement; $B(r, t)$ the magnetic induction; $H(r, t)$ the magnetic field; $J^e(r, t)$ the electric current density; $J^m(r, t)$ the magnetic current density; $\rho^e(r, t)$ the electric charge density; $\rho^m(r, t)$ the magnetic charge density; (r, t) a space–time point; ∇ the del operator; and c represents the speed of light in vacuum. Both magnetic charge and current densities (Magid, 1972) have been included in Maxwell's equations for purposes of completeness. They, of course, can be set equal to zero since magnetic charge has not been discovered in nature. The electric displacement and electric field vectors, as well as the magnetic induction and magnetic field vectors, are related (Jackson, 1962) through the mathematical expressions

$$D(r, t) = E(r, t) + 4\pi P(r, t) \tag{5}$$

and

$$B(r, t) = H(r, t) + 4\pi M(r, t), \tag{6}$$

where $P(r, t)$ and $M(r, t)$ are the macroscopic polarization and magnetization vectors.

The Maxwell field equations (1) through (4), with the use of equations (5) and (6), can be cast (Bocker, 1992) into the following covariant matrix equation

$$\begin{bmatrix} M_1 & M_2 \\ M_2 & M_1 \end{bmatrix} \begin{bmatrix} f_1 \\ f_2 \end{bmatrix} + 4\pi \begin{bmatrix} M_1 & O \\ O & M_1 \end{bmatrix} \begin{bmatrix} d_1 \\ d_2 \end{bmatrix} = \frac{4\pi}{c} \begin{bmatrix} s_1 \\ s_2 \end{bmatrix}. \tag{7}$$

This matrix representation of the Maxwell field equations forms the basis for all other work described in this report. For the Lorentz gauge choice (Bocker & Frieden, 1992), the 4 by 4 differential matrix operators $[M_1]$ and $[M_2]$ are defined by the equation

$$[M_1] \equiv \begin{bmatrix} -\frac{\partial}{\partial \tau} & 0 & 0 & -\frac{\partial}{\partial x} \\ 0 & -\frac{\partial}{\partial \tau} & 0 & -\frac{\partial}{\partial y} \\ 0 & 0 & -\frac{\partial}{\partial \tau} & -\frac{\partial}{\partial z} \\ \frac{\partial}{\partial x} & \frac{\partial}{\partial y} & \frac{\partial}{\partial z} & -\frac{\partial}{\partial \tau} \end{bmatrix} \quad and \quad [M_2] \equiv \begin{bmatrix} 0 & -\frac{\partial}{\partial z} & \frac{\partial}{\partial y} & 0 \\ \frac{\partial}{\partial z} & 0 & -\frac{\partial}{\partial x} & 0 \\ -\frac{\partial}{\partial y} & \frac{\partial}{\partial x} & 0 & 0 \\ 0 & 0 & 0 & 0 \end{bmatrix} \tag{8}$$

3

where

$$r = (x, y, z) \qquad and \qquad \tau = ict. \tag{9}$$

The imaginary quantity i is equal to $\sqrt{-1}$. The matrix $[O]$ in equation (7) represents the 4 by 4 null matrix. The 4 by 1 electric and magnetic field vectors $[f_1]$ and $[f_2]$ appearing in equation (7) are defined by

$$\left[f_1\right] \equiv i \begin{bmatrix} E_x \\ E_y \\ E_z \\ 0 \end{bmatrix} \qquad and \qquad \left[f_2\right] \equiv \begin{bmatrix} H_x \\ H_y \\ H_z \\ 0 \end{bmatrix}. \tag{10}$$

The 4 by 1 polarization and magnetization vectors $[d_1]$ and $[d_2]$ are defined by

$$\left[d_1\right] \equiv i \begin{bmatrix} P_x \\ P_y \\ P_z \\ 0 \end{bmatrix} \qquad and \qquad \left[d_2\right] \equiv \begin{bmatrix} M_x \\ M_y \\ M_z \\ 0 \end{bmatrix}. \tag{11}$$

The electric and magnetic source vectors $[s_1]$ and $[s_2]$ appearing in equation (7) are relativistic 4-vectors defined by

$$\left[s_1\right] \equiv \begin{bmatrix} J_x^e \\ J_y^e \\ J_z^e \\ ic\rho^e \end{bmatrix} \qquad and \qquad \left[s_2\right] \equiv -i \begin{bmatrix} J_x^m \\ J_y^m \\ J_z^m \\ ic\rho^m \end{bmatrix}. \tag{12}$$

It is through the polarization, magnetization, and source vectors that the material characteristics of the medium are mathematically described. As previously indicated, our interest concerns dielectric, i.e., linear, homogeneous, isotropic, and conductive materials only.

4

2.2 DIELECTRIC MEDIUM

For a linear medium, the polariz⁻ .on and magnetization vectors, $[d_1]$ and $[d_2]$, are related to the electric and magnet⁻ field vectors, $[f_1]$ and $[f_2]$, by the matrix equation

$$\begin{bmatrix} d_1 \\ d_2 \end{bmatrix} = \begin{bmatrix} \chi_e & O \\ O & \chi_m \end{bmatrix} \begin{bmatrix} f_1 \\ f_2 \end{bmatrix} \tag{13}$$

where $[\chi_e]$ and $[\chi_m]$ are the 4 by 4 electric and magnetic susceptibility tensors (matrices) respectively. Substitution of equation (13) back into equation (7) gives

$$\begin{bmatrix} M_1 & M_2 \\ M_2 & M_1 \end{bmatrix} \begin{bmatrix} f_1 \\ f_2 \end{bmatrix} + 4\pi \begin{bmatrix} M_1 & O \\ O & M_1 \end{bmatrix} \begin{bmatrix} \chi_e & O \\ O & \chi_m \end{bmatrix} \begin{bmatrix} f_1 \\ f_2 \end{bmatrix} = \frac{4\pi}{c} \begin{bmatrix} s_1 \\ s_2 \end{bmatrix}. \tag{14}$$

The 4 by 4 dielectric and permeability matrices, $[\varepsilon]$ and $[\mu]$, are related to the electric and magnetic susceptibility matrices by the equations

$$[\varepsilon] \equiv [I] + 4\pi [\chi_e] \tag{15}$$

and

$$[\mu] \equiv [I] + 4\pi [\chi_m] \tag{16}$$

where $[I]$ is the 4 by 4 identity matrix. With the use of equations (15) and (16), matrix equation (14) can be written in the form

$$\begin{bmatrix} M_1\varepsilon & M_2 \\ M_2 & M_1\mu \end{bmatrix} \begin{bmatrix} f_1 \\ f_2 \end{bmatrix} = \frac{4\pi}{c} \begin{bmatrix} s_1 \\ s_2 \end{bmatrix}. \tag{17}$$

For a medium having electrical conductive properties, the electric source vector $[s_1]$ appearing in equation (17) obeys Ohm's law

$$\begin{bmatrix} s_1 \\ s_2 \end{bmatrix} = \begin{bmatrix} -i\sigma & O \\ O & O \end{bmatrix} \begin{bmatrix} f_1 \\ f_2 \end{bmatrix} \tag{18}$$

where $[\sigma]$ is the 4 by 4 electrical conductivity matrix. Note, in the absence of magnetic charge, the magnetic source vector $[s_2]$ may be set equal to zero. With the use of equation (18), matrix equation (17) can be written in the form

$$
\begin{bmatrix}
M_1 \varepsilon + i\gamma & M_2 \\
M_2 & M_1 \mu
\end{bmatrix}
\begin{bmatrix}
f_1 \\
f_2
\end{bmatrix}
=
\begin{bmatrix}
o \\
o
\end{bmatrix}
\tag{19}
$$

where $[o]$ is a 4 by 1 null vector and where by definition

$$
[\gamma] \equiv \frac{4\pi}{c} [\sigma] .
\tag{20}
$$

Equation (19) is the matrix representation of the Maxwell field equations for a linear, conductive medium of infinite extent. If the medium is isotropic and homogeneous as well, the 4 by 4 matrices $[\varepsilon]$, $[\mu]$, and $[\sigma]$ appearing in equations (19) and (20) have the simplified diagonal form

$$
[\varepsilon] =
\begin{bmatrix}
\varepsilon & 0 & 0 & 0 \\
0 & \varepsilon & 0 & 0 \\
0 & 0 & \varepsilon & 0 \\
0 & 0 & 0 & \varepsilon
\end{bmatrix},
\qquad
[\mu] =
\begin{bmatrix}
\mu & 0 & 0 & 0 \\
0 & \mu & 0 & 0 \\
0 & 0 & \mu & 0 \\
0 & 0 & 0 & \mu
\end{bmatrix},
\qquad
[\sigma] =
\begin{bmatrix}
\sigma & 0 & 0 & 0 \\
0 & \sigma & 0 & 0 \\
0 & 0 & \sigma & 0 \\
0 & 0 & 0 & \sigma
\end{bmatrix}.
\tag{21}
$$

For this case, all of the nonzero main-diagonal elements in each of these 4 by 4 matrices are equal to a scalar constant, which is independent of position and time. Hence, the dielectric medium being considered here may be simply described by the three scalar constants ε, μ, σ.

2.3 MULTILAYER DIELECTRIC MEDIUM

We now consider the geometry shown in figure 1. This figure depicts a multilayer optical medium consisting of N layers sandwiched between a left and right semi-infinite subregion of space. Each layer represents a dielectric subregion of space. Adjacent layers are separated by parallel planar interface boundaries orthogonal to the z-axis. The multilayer medium is illuminated by an electromagnetic wave incident from the left. This gives rise to both a reflected and a transmitted electromagnetic wave. The principal objective in solving a problem of this nature is to determine the characteristics of the reflected and transmitted waves in terms of the properties of the incident wave as well as the optical and geometrical properties of the multilayer medium.
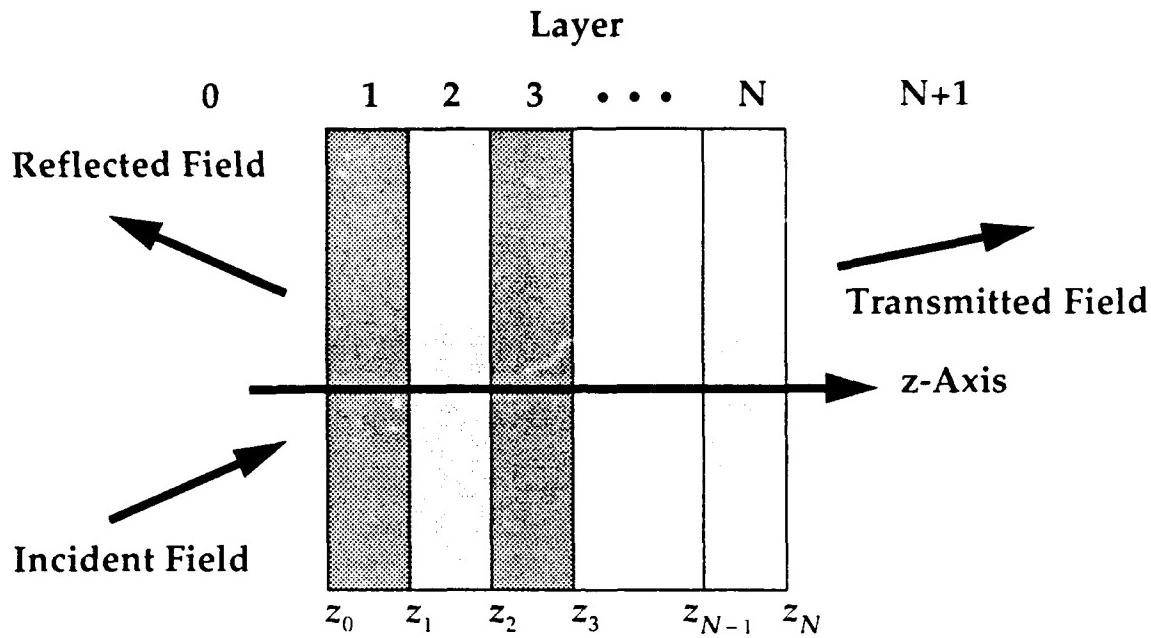
Figure 1. Multilayer geometry.

For a multilayer optical medium, the three matrices appearing in equation (21) are now a function of the spatial coordinate z. We can write these matrices in the form

$$[\varepsilon] = \sum_{n=0}^{N+1} [\varepsilon]_n \Psi_n(z) \tag{22}$$

$$[\mu] = \sum_{n=0}^{N+1} [\mu]_n \Psi_n(z) \tag{23}$$

$$[\sigma] = \sum_{n=0}^{N+1} [\sigma]_n \Psi_n(z). \tag{24}$$

7

The matrices $[\varepsilon]_n$, $[\mu]_n$, and $[\sigma]_n$ represent the dielectric, permeability, and conductivity matrices associated with subregion n. The functions $\Psi_n(z)$, hereafter denoted partition functions, are used in partitioning space into the various subregions depicted in figure 1. These partition functions are defined in terms of the Heaviside step function (Bracewell, 1965). The reader is referred to appendix A, which contains a more detailed description of the partition functions as well as their properties.

The electromagnetic field vector appearing in equation (19) may also be partitioned in a similar manner. That is,

$$\begin{bmatrix} f_1 \\ f_2 \end{bmatrix} = \sum_{n=0}^{N+1} \begin{bmatrix} f_1 \\ f_2 \end{bmatrix}_n \Psi_n(z) \tag{25}$$

where $[f_1 \ f_2]_n^T$ is the electromagnetic field vector associated with subregion n. The superscript T refers to transpose. Next, we substitute equations (22) through (25) back into equation (19). Using the multiplicative property (see appendix A) of the partition functions $\Psi_n(z)$ gives the following matrix representation of the Maxwell field equations for a dielectric multilayer optical medium

$$\sum_{n=0}^{N+1} \begin{bmatrix} M_1\varepsilon + i\gamma & M_2 \\ M_2 & M_1\mu \end{bmatrix}_n \left\{ \begin{bmatrix} f_1 \\ f_2 \end{bmatrix}_n \Psi_n(z) \right\} = \begin{bmatrix} 0 \\ 0 \end{bmatrix} \tag{26}$$

where by definition

$$\begin{bmatrix} M_1\varepsilon + i\gamma & M_2 \\ M_2 & M_1\mu \end{bmatrix}_n \equiv \begin{bmatrix} M_1\varepsilon_n + i\gamma_n & M_2 \\ M_2 & M_1\mu_n \end{bmatrix}. \tag{27}$$

Notice the similarity between the matrix form (26) of the Maxwell field equations for a multilayer medium and the matrix form (19) for an infinite medium without boundaries. Next, we will show that the matrix representation (26) of the Maxwell field equations for a multilayer medium has the electromagnetic boundary conditions built into the representation. There is no need to consider the use of the Divergence Theorem and Stoke's Theorem in establishing the boundary conditions of the electromagnetic fields at the various planar interfaces.

With the use of the product rule from calculus (Wylie, 1953), equation (26) takes on the following form

$$\sum_{n=0}^{N+1} \Psi_n(z) \begin{bmatrix} M_1\varepsilon + i\gamma & M_2 \\ M_2 & M_1\mu \end{bmatrix}_n \begin{bmatrix} f_1 \\ f_2 \end{bmatrix}_n + \sum_{n=0}^{N+1} \Phi_n(z) \begin{bmatrix} C_1\varepsilon & C_2 \\ C_2 & C_1\mu \end{bmatrix}_n \begin{bmatrix} f_1 \\ f_2 \end{bmatrix}_n = \begin{bmatrix} 0 \\ 0 \end{bmatrix} \qquad (28)$$

where from appendix A

$$\Phi_n(z) \equiv \frac{d}{dz}\Psi_n(z). \qquad (29)$$

The matrices $[C_1]$ and $[C_2]$ appearing in equation (28) are given by

$$[C_1] = \begin{bmatrix} 0 & 0 & 0 & 0 \\ 0 & 0 & 0 & 0 \\ 0 & 0 & 0 & -1 \\ 0 & 0 & +1 & 0 \end{bmatrix} \quad and \quad [C_2] = \begin{bmatrix} 0 & -1 & 0 & 0 \\ +1 & 0 & 0 & 0 \\ 0 & 0 & 0 & 0 \\ 0 & 0 & 0 & 0 \end{bmatrix}. \qquad (30)$$

With the use of equations (A.5), (A.6), and (A.7) from appendix A, we can rewrite equation (28) in the form

$$\sum_{n=0}^{N+1} \Psi_n(z) \begin{bmatrix} M_1\varepsilon + i\gamma & M_2 \\ M_2 & M_1\mu \end{bmatrix}_n \begin{bmatrix} f_1 \\ f_2 \end{bmatrix}_n \qquad (31)$$

$$+ \sum_{p=0}^{N} \delta(z-z_p) \left\{ \begin{bmatrix} C_1\varepsilon & C_2 \\ C_2 & C_1\mu \end{bmatrix}_{p+1} \begin{bmatrix} f_1 \\ f_2 \end{bmatrix}_{p+1} - \begin{bmatrix} C_1\varepsilon & C_2 \\ C_2 & C_1\mu \end{bmatrix}_{p} \begin{bmatrix} f_1 \\ f_2 \end{bmatrix}_{p} \right\} = \begin{bmatrix} 0 \\ 0 \end{bmatrix}.$$

It is of interest to note that the first sum appearing in equation (31) is nothing more than a mathematical statement of the fact that the Maxwell field equations must be satisfied for each dielectric subregion n, $(n = 0, 1, 2, ..., N+1)$. The second sum appearing in equation (31) contains the boundary conditions that must be satisfied at each planar interface boundary $z = z_p$, $(p = 0, 1, 2, ..., N)$ separating the various subregions of

9

space. For equation (31) to be satisfied at all points in space, the following two sets of matrix equations must be satisfied:

Maxwell field equations in each subregion n

$$\begin{bmatrix} M_1\varepsilon + i\gamma & M_2 \\ M_2 & M_1\mu \end{bmatrix}_n \begin{bmatrix} f_1 \\ f_2 \end{bmatrix}_n = \begin{bmatrix} o \\ o \end{bmatrix} \qquad (n = 0, 1, 2, \ldots N + 1) \qquad (32)$$

Boundary conditions at each planar interface $z = z_p$

$$\begin{bmatrix} C_1\varepsilon & C_2 \\ C_2 & C_1\mu \end{bmatrix}_p \begin{bmatrix} f_1 \\ f_2 \end{bmatrix}_p = \begin{bmatrix} C_1\varepsilon & C_2 \\ C_2 & C_1\mu \end{bmatrix}_{p+1} \begin{bmatrix} f_1 \\ f_2 \end{bmatrix}_{p+1} \qquad (p = 0, 1, 2, \ldots, N). \qquad (33)$$

Next, we will consider the case of monochromatic plane-wave solutions. Appendix B contains a detailed mathematical discussion on monochromatic plane-wave solutions of matrix equation (19), or equivalently matrix equation (32), and their resulting properties. In addition, appendix C contains a detailed mathematical discussion on the boundary condition equation (33) for the case of monochromatic plane-wave solutions. It is highly advisable at this point for the reader to become familiar with the concepts and notation presented in these appendices before continuing on.

2.4 ELECTROMAGNETIC PLANE-WAVE FIELDS

Suppose the dielectric multilayer optical medium depicted in figure 1 is illuminated by a monochromatic electromagnetic plane-wave, hereafter referred to as simply the incident wave. The incident wave will give rise to both a transmitted and a reflected monochromatic electromagnetic plane-wave as shown in figure 1. In addition, as a result of the incident wave excitation, each layer within the multilayer medium will support two monochromatic electromagnetic plane-waves propagating in opposite directions (Fowles, 1968). Therefore, the electromagnetic field vectors appearing in equations (32) and (33) must be of the form

$$\begin{bmatrix} f_1 \\ f_2 \end{bmatrix} = \begin{bmatrix} f_1 \\ f_2 \end{bmatrix}_R + \begin{bmatrix} f_1 \\ f_2 \end{bmatrix}_L \qquad (34)$$

10

where each of the field vectors on the right-hand side of equation (34) has a monochromatic plane-wave representation given by equation (B.2) in appendix B, namely

$$\begin{bmatrix} f_1 \\ f_2 \end{bmatrix}_R = \begin{bmatrix} f_{01} \\ f_{02} \end{bmatrix}_R exp\{i[r]^T[k]_R\} \tag{35}$$

$$\begin{bmatrix} f_1 \\ f_2 \end{bmatrix}_L = \begin{bmatrix} f_{01} \\ f_{02} \end{bmatrix}_L exp\{i[r]^T[k]_L\}. \tag{36}$$

The subscripts R and L appearing in equations (34) through (36) denote wave propagation to the right and left respectively. Substitution of equation (34) back into equation (33), with the use of equations (35) and (36), gives the following equation

$$\begin{bmatrix} G_1 & O \\ O & G_2 \end{bmatrix}_p \left\{ \begin{bmatrix} f_{01} \\ f_{02} \end{bmatrix}_R exp(+iz_pk_z) + \begin{bmatrix} f_{01} \\ f_{02} \end{bmatrix}_L exp(-iz_pk_z) \right\}_p = \tag{37}$$

$$\begin{bmatrix} G_1 & O \\ O & G_2 \end{bmatrix}_{p+1} \left\{ \begin{bmatrix} f_{01} \\ f_{02} \end{bmatrix}_R exp(+iz_pk_z) + \begin{bmatrix} f_{01} \\ f_{02} \end{bmatrix}_L exp(-iz_pk_z) \right\}_{p+1}.$$

The mathematical details le ·ding up to equation (37) are presented in appendix C. The above 4 by 4 matrices $[G_1]$ and $[G_2]$ are given by equation (C-4).

The electric field vector $[f_{01}]$ and magnetic field vector $[f_{02}]$ appearing in equation (37) are not independent, but are in fact related to one another through equation (B.20) in appendix B. With the use of equation (B.20), we can eliminate the magnetic field vectors, for example, from equation (37). Doing so allows us to cast equation (37) into the following matrix form

$$\begin{bmatrix} S_{11}(z_p) & S_{12}(z_p) \\ S_{21}(z_p) & S_{22}(z_p) \end{bmatrix}_p \begin{bmatrix} [f_{01}]_R \\ [f_{01}]_L \end{bmatrix}_p = \begin{bmatrix} S_{11}(z_p) & S_{12}(z_p) \\ S_{21}(z_p) & S_{22}(z_p) \end{bmatrix}_{p+1} \begin{bmatrix} [f_{01}]_R \\ [f_{0}·]_L \end{bmatrix}_{p+1} \tag{38}$$

11

where

$$
\begin{bmatrix} S_{11}(z) & S_{12}(z) \\ S_{21}(z) & S_{22}(z) \end{bmatrix} \equiv \begin{bmatrix} G_1 F_1(z) & G_1 F_2(z) \\ G_2 F_1(z) R & G_2 F_2(z) L \end{bmatrix} \tag{39}
$$

and

$$
[F_1(z)] \equiv [I] \exp(+izk_z) \qquad and \qquad [F_2(z)] \equiv [I] \exp(-izk_z) \tag{40}
$$

$$
[R] \equiv -i\sqrt{\frac{\hat{\varepsilon}}{\mu}} [\alpha_1 + \alpha_2]_R \qquad and \qquad [L] \equiv -i\sqrt{\frac{\hat{\varepsilon}}{\mu}} [\alpha_1 + \alpha_2]_L \tag{41}
$$

The matrix $[I]$ in equation (40) is again the 4 by 4 identity matrix. The 4 by 4 direction cosine matrices $[\alpha_1]$ and $[\alpha_2]$ are defined by equation (B.9) in appendix B. The quantity $\hat{\varepsilon}$ is the complex dielectric constant, also defined in appendix B. Matrix equation (38) summarizes the relationship between the electric field vectors associated with the electromagnetic waves propagating to the right and the left in layers p and $p+1$ evaluated at the planar interface $z = z_p$.

2.5 MULTILAYER SYSTEM MATRIX OPERATOR

We will next generate a multilayer system matrix operator that will ultimately allow us to determine the mathematical relationship between the incident, reflected, and transmitted waves depicted in figure 1. First, we define a new 8 by 8 matrix involving the 8 by 8 matrices in equation (38), namely

$$
\begin{bmatrix} \Lambda_{11}(z_p) & \Lambda_{12}(z_p) \\ \Lambda_{21}(z_p) & \Lambda_{22}(z_p) \end{bmatrix}_{p+1,p} \equiv \begin{bmatrix} S_{11}(z_p) & S_{12}(z_p) \\ S_{21}(z_p) & S_{22}(z_p) \end{bmatrix}_{p+1}^{-1} \begin{bmatrix} S_{11}(z_p) & S_{12}(z_p) \\ S_{21}(z_p) & S_{22}(z_p) \end{bmatrix}_p . \tag{42}
$$

The superscript, -1, denotes the multiplicative matrix inverse operation. Equation (38) can now be rewritten in the form

$$
\begin{bmatrix} [f_{01}]_R \\ [f_{01}]_L \end{bmatrix}_{p+1} = \begin{bmatrix} \Lambda_{11}(z_p) & \Lambda_{12}(z_p) \\ \Lambda_{21}(z_p) & \Lambda_{22}(z_p) \end{bmatrix}_{p+1,p} \begin{bmatrix} [f_{01}]_R \\ [f_{01}]_L \end{bmatrix}_p . \tag{43}
$$

12

Equation (43) allows us to calculate the electric field vectors in subregion $p+1$ in terms of the electric field vectors in subregion p. The multilayer system matrix operator can now be computed through successive matrix multiplications leading to the following equation

$$
\begin{bmatrix} \Gamma_{11} & \Gamma_{12} \\ \Gamma_{21} & \Gamma_{22} \end{bmatrix}_{sys} = \prod_{p=N}^{0} \begin{bmatrix} \Lambda_{11}(z_p) & \Lambda_{12}(z_p) \\ \Lambda_{21}(z_p) & \Lambda_{22}(z_p) \end{bmatrix}_{p+1,\,p} . \tag{44}
$$

With the use of the above multilayer system matrix operator, we can now express the electric field vectors in the right semi-infinite subregion $N+1$ in terms of the electric field vectors in left semi-infinite subregion 0. The result is

$$
\begin{bmatrix} [f_{01}]_R \\ [f_{01}]_L \end{bmatrix}_{N+1} = \begin{bmatrix} \Gamma_{11} & \Gamma_{12} \\ \Gamma_{21} & \Gamma_{22} \end{bmatrix}_{sys} \begin{bmatrix} [f_{01}]_R \\ [f_{01}]_L \end{bmatrix}_{0} . \tag{45}
$$

For simplicity in notation we let

$$
[f_i] = [\,[f_{01}]_R\,]_0 \tag{46}
$$

$$
[f_r] = [\,[f_{01}]_L\,]_0 \tag{47}
$$

$$
[f_t] = [\,[f_{01}]_R\,]_{N+1} . \tag{48}
$$

The three vectors in equations (46), (47), and (48) represent the incident, reflected, and transmitted electric field vectors respectively. Based on the illumination scenario depicted in figure 1, there is no electromagnetic wave in subregion $N+1$ propagating to the left, hence

$$
[\,[f_{01}]_L\,]_{N+1} = [o] . \tag{49}
$$

With the use of equations (46) through (49), we can now rewrite equation (45) in the form

$$
\begin{bmatrix} f_t \\ o \end{bmatrix} = \begin{bmatrix} \Gamma_{11} & \Gamma_{12} \\ \Gamma_{21} & \Gamma_{22} \end{bmatrix}_{sys} \begin{bmatrix} f_i \\ f_r \end{bmatrix} . \tag{50}
$$

13

With the use of equation (50), we can now solve for the reflected and the transmitted electric field vectors in terms of the incident electric field vector. We obtain the result

$$[f_r] = -[\ \Gamma_{22}^{-1}\ \Gamma_{21}\ ]_{sys}\ [f_i] \tag{51}$$

$$[f_t] = +[\ \Gamma_{11} - \Gamma_{12}\ \Gamma_{22}^{-1}\ \Gamma_{21}\ ]_{sys}\ [f_i]. \tag{52}$$

The reflectance, $\mathcal{R}$, and transmittance, $\mathcal{T}$, coefficients (Born & Wolf. 1965) of the multilayer medium can now be computed using the following equations

$$\mathcal{R} = \frac{[f_r]^H\ [f_r]}{[f_i]^H\ [f_i]} \tag{53}$$

$$\mathcal{T} = \frac{[f_t]^H\ [f_t]\ n_t\ \cos(\theta_t)}{[f_i]^H\ [f_i]\ n_i\ \cos(\theta_i)}. \tag{54}$$

The superscript, H, denotes the Hermitian conjugate operation. The quantities n_i and n_t correspond to the ordinary indices of refraction for subregions 0 and $N + 1$ respectively. The angles θ_i and θ_t represent the angle of incidence and angle of refraction for the subregions 0 and $N + 1$ respectively. These angles and indices of refraction obey the Snell's law relation

$$n_i \sin(\theta_i) = n_t \sin(\theta_t). \tag{55}$$

Equation (54) tacitly assumes that the subregions 0 and $N+1$ are nonconducting. Typically these two subregions correspond to either vacuum, air, or glass. There are no restrictions placed on the optical properties of the dielectric layers constituting the multilayer medium. Equations (53) and (54) are the quintessential equations necessary for calculating the reflection and transmission characteristics of the multilayer medium. It is noted that the wavelength, angle of incidence, and polarization state of the incident wave can be arbitrarily chosen. These equations serve as the basis for the applications considered in the following section.

3.0 APPLICATIONS

Based on the 8 by 8 matrix representation of electromagnetic theory being developed by the author, a computer software package is currently being written and tested at NRaD to handle a variety of scenarios involving electromagnetic wave propagation through matter. This software package is referred to as the MATURE Program. MATURE is the acronym for Matrix Approach To Understanding Relativistic Electrodynamics. MATURE is written in MATLAB code for a Sun 4 SPARCstation 2 workstation. One feature of the MATURE Program is its ability to solve electromagnetic wave propagation problems involving multilayer optical structures. The required inputs to the MATURE Program for problems of this nature are based on the following statements:

1. Enter total number of optical layers, N.
2. Enter thickness, T_p, of each layer in nanometers (nm) for $p = 1, 2,..., N$.
3. Enter ordinary refractive index, n_p, of each subregion $p = 0, 1, 2,..., N, N+1$.
4. Enter attenuation index, κ_p, of each subregion $p = 0, 1, 2,..., N, N+1$.
5. Enter angle of incidence, θ_i, of incident plane-wave in degrees (deg).
6. Enter wavelength, λ, of incident plane-wave in nm.
7. Specify polarization state, Transverse Electric (TE) or Transverse Magnetic (TM), of incident plane-wave.
8. Determine the variable of interest, namely wavelength, λ, angle of incidence, θ_i, or thickness, T_n, of the nth layer.
9. If the variable of interest is the wavelength, then
   a. Specify minimum value of wavelength, λ_{min}, in nm,
   b. Specify maximum value of wavelength, λ_{max}, in nm,
   c. Specify incremental value of wavelength, $\Delta\lambda$, in nm.
10. If the variable of interest is the angle of incidence, then
   a. Specify minimum value of angle of incidence, $\theta_{i, min}$, in deg,
   b. Specify maximum value of angle of incidence, $\theta_{i, max}$, in deg,
   c. Specify incremental value of angle of incidence, $\Delta\theta_i$, in deg.
11. If the variable of interest is the thickness of the nth layer, then
   a. Specify layer number, n, of interest,
   b. Specify minimum thickness, $T_{n, min}$, of nth layer in nm,
   c. Specify maximum thickness, $T_{n, max}$, of nth layer in nm,
   d. Specify incremental thickness, ΔT_n, of nth layer in nm.

The outputs to the MATURE Program are the reflectance, $\mathcal{R}$, and transmittance, $\mathcal{T}$, as a function of the variable of interest.

With the use of the MATURE Program, a number of examples are considered in this section that illustrate the utility of the 8 by 8 matrix representation in solving electromagnetic wave propagation problems involving multilayer optical media. The examples considered involve: (1) reflection and refraction at a single interface separating two nonconducting dielectric media, (2) evanescent wave coupling from one dielectric medium into another via a vacuous thin film, (3) the reflection and transmission properties of a single conducting metal thin film, (4) the reflection and transmission characteristics of a multilayer antireflection coating structure, (5) the reflection and transmission properties of a multilayer high-reflectance mirror, and (6) the reflection and transmission characteristics of a multilayer interference band-pass filter.

3.1 SINGLE SURFACE REFLECTION AND REFRACTION

For our first example we consider reflection and refraction at a planar interface separating two nonconducting dielectric media. This corresponds to a geometry in which $N = 0$ in figure 1. It is convenient to consider two special cases. The first case is that in which the electric field vector of the incident wave is parallel to the planar interface. This is commonly referred to as the transverse electric or TE polarization case. The second case is that in which the magnetic field vector of the incident wave is parallel to the interface. This is known as the transverse magnetic or TM polarization case. The general case is handled by using appropriate linear combinations of these two special cases. Figure 2 shows the results obtained from the MATURE Program for a rare-to-dense (external reflection) scenario (Fowles, 1968). The left semi-infinite subregion of space in figure 1 is a vacuum and the right semi-infinite subregion is a nonconducting medium with ordinary refractive index equal to 1.5. The wavelength of the incident wave was 500 nm and the angle of incidence was chosen as the variable of interest. It is apparent from figure 2 that, for the TM case, the reflectance is zero at the Brewster angle (polarization angle) value of 56.3° predicted by

$$\theta_b = \text{atan}\left[\frac{n_1}{n_0}\right] = \text{atan}\left[\frac{1.5}{1.0}\right]. \tag{56}$$

Also note that the reflectance at $\theta_i = 0°$ is equal to 4 percent, which is in agreement with the formula

$$\mathcal{R} = \left[\frac{n_1 - n_0}{n_1 + n_0}\right]^2 \tag{57}$$

used to predict (Fowles, 1968) reflectance at normal incidence. Figure 3 illustrates the results obtained for a dense-to-rare (internal reflection) scenario (Fowles, 1968). For this

REGION	THICKNESS (nm)	REFRACTIVE INDEX	ATTENUATION INDEX
LEFT		1.000	0.000
RIGHT		1.500	0.000

Wavelength: 500.0 (nm)

REFLECTANCE (%)

TRANSMITTANCE (%)
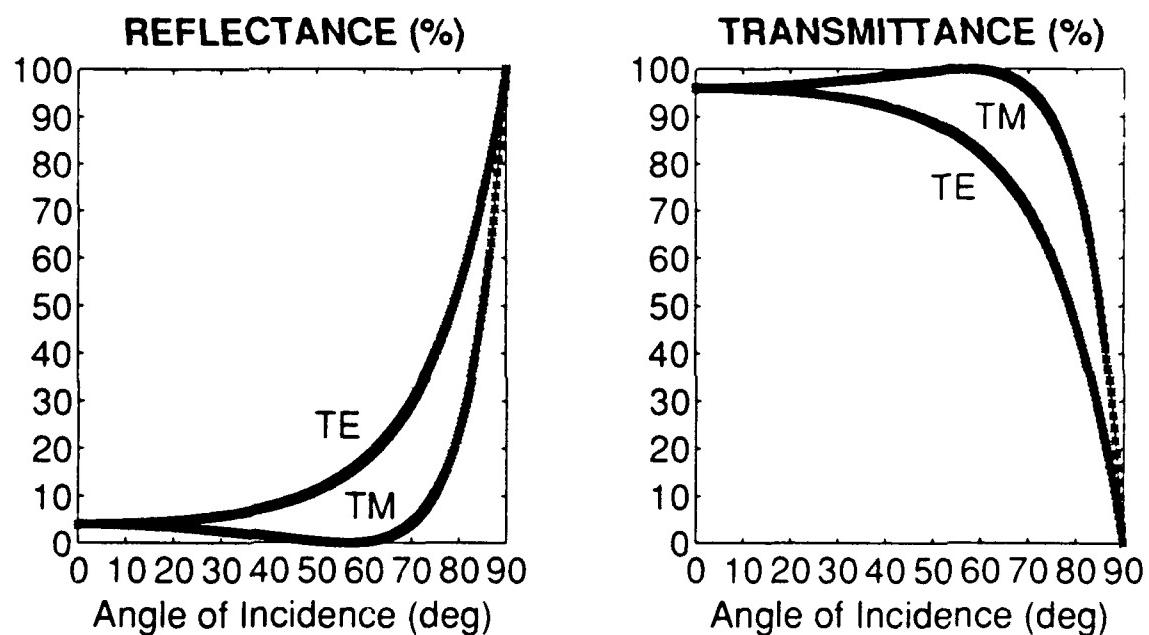
Figure 2. Single surface (rare-to-dense).

REGION	THICKNESS (nm)	REFRACTIVE INDEX	ATTENUATION INDEX
LEFT		1.500	0.000
RIGHT		1.000	0.000

Wavelength: 500.0 (nm)

REFLECTANCE (%)

TRANSMITTANCE (%)

Angle of Incidence (deg)

Angle of Incidence (deg)
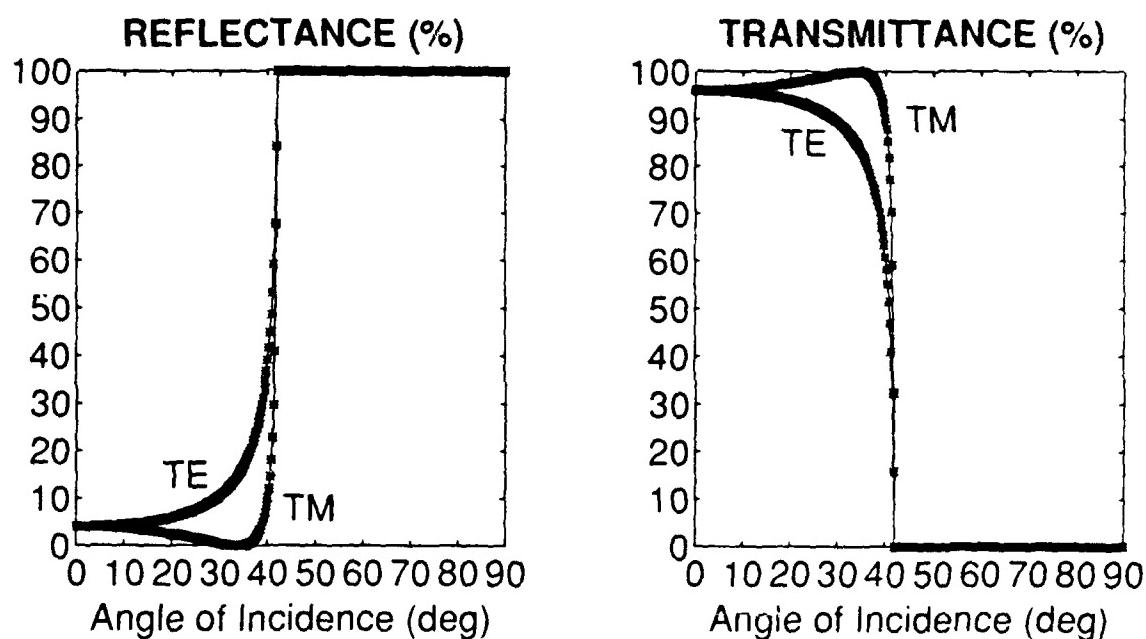
Figure 3. Single surface (dense-to-rare).

scenario, the right semi-infinite subregion of space is a vacuum and the left semi-infinite subregion is a nonconducting medium with ordinary refractive index equal to 1.5. Again, the wavelength was set equal 500 nm in the MATURE Program and the angle of incidence was chosen as the variable of interest. The Brewster angle for this scenario is equal to 33.7°. The reflectance at normal incidence is again 4 percent. In addition, we observe that total internal reflectance occurs for angles of incidence greater than the critical angle (Fowles, 1968) of 41.8° predicted by the formula

$$\theta_c = \text{asin}\left[\frac{n_1}{n_0}\right] = \text{asin}\left[\frac{1.0}{1.5}\right]. \tag{58}$$

The reflectance and transmittance plots in both figures 2 and 3 are in excellent agreement with results found in standard textbooks on optics, e.g., Born & Wolf (1965) and Fowles (1968), treating this subject.

3.2 EVANESCENT WAVE COUPLING

In the next example, we consider the transport of electromagnetic energy between two semi-infinite nonconducting dielectric media separated by a vacuous thin film. This corresponds to $N = 1$ in the geometry of figure 1. For this example, the ordinary refractive index of each dielectric medium was set equal to 1.5. The wavelength of the incident wave was set equal to 500 nm. Only the TE polarization case was considered. The thickness of the vacuous thin film was varied between 0 and 1000 nm. Three different test cases were considered corresponding to angles of incidence of 0°, 38°, and 45°, respectively. Figure 4 summarizes the results obtained using the MATURE Program. Note that the critical angle for this example is equal to 41.8°. For angles of incidence less than the critical angle, the vacuous thin film behaves as an optical cavity. The periodic variations in both the reflectance and transmittance of the multilayer optical structure, with thin-film thickness, is clearly obvious from the plots in figure 4. However, for angles of incidence exceeding the critical angle, the periodic behavior of the reflectance and transmittance of the multilayer structure ceases. This periodic behavior has been replaced by an exponential decrease (increase) in the transmittance (reflectance) of the multilayer structure with increasing values of the thin-film thickness. Notice how the optical structure becomes totally reflecting for all practical purposes beyond a thin-film thickness of about 600 nm when the angle of incidence is equal to 45°. The behavior of a structure of this nature for angles of incidence exceeding the critical angle is attributed to a phenomena called evanescent wave coupling. For a detailed discussion on evanescent wave coupling, the reader is referred to Fowles (1968).

REGION	THICKNESS (nm)	REFRACTIVE INDEX	ATTENUATION INDEX
LEFT		1.500	0.000
1	1000.0	1.000	0.000
RIGHT		1.500	0.000

Incidence Angle: 0, 38, 45 (deg)   Wavelength: 500.0 (nm)

REFLECTANCE (%)

TRANSMITTANCE (%)
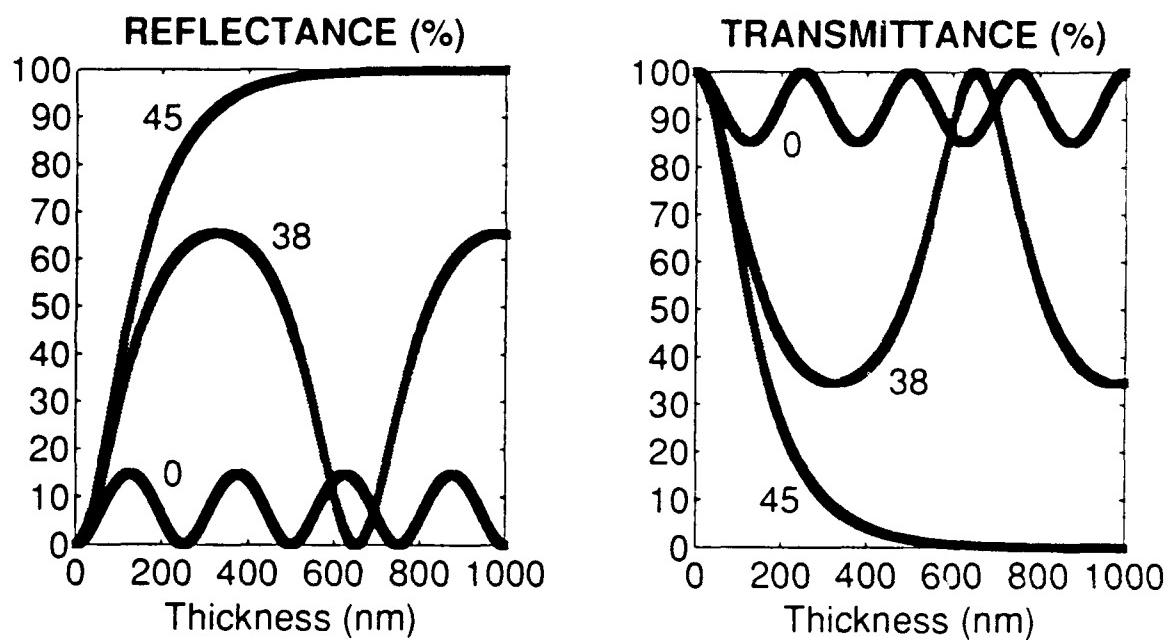
Figure 4. Vacuous thin film (TE polarization).

3.3 SINGLE CONDUCTING THIN FILM

For our next example, we consider a multilayer optical medium consisting of a single conducting metallic thin film separating two semi-infinite dielectric subregions of space. This corresponds to $N = 1$ in the geometry of figure 1. There are two scenarios we wish to consider. In the first scenario, the left semi-infinite subregion of space in figure 1 is a vacuum and the right semi-infinite subregion is a dielectric medium with ordinary refractive index equal to 1.5. The ordinary refractive index of the metal film is 3.5. The attenuation index of the metallic thin film was set equal to three different values, namely 0.0, 0.1, and 0.2. The thin-film structure was normally illuminated by a plane-wave of wavelength 500 nm. For normal incidence there is no distinction between the TE and TM polarization cases. The variable of interest was the thin-film thickness. The thickness was varied between 0 and 300 nm. In figures 5, 6, and 7 are plots of the reflectance and transmittance of the metallic thin-film structure as a function of thin-film thickness for the attenuation index values of 0.0, 0.1, and 0.2 respectively. The results summarized in these three figures are in excellent agreement with similar results reported by Born and Wolf (1965).

The second scenario considered involves a metallic thin film separating two vacuous semi-infinite subregions of space. The ordinary refractive and attenuation index values, (n_1, κ_1), chosen for the thin film correspond to values for real metals. In particular, the following metals were considered: silver (0.200, 17.200); aluminum (1.440, 3.632); gold (0.470, 6.021); copper (0.620, 4.145); and iron (1.510, 1.079). The thin-film structure was illuminated at normal incidence by a plane-wave of wavelength 589.3 nm. The variable of interest was the thickness of the thin film that was varied between 0 and 100 nm. Results obtained for the five metallic thin films considered are shown in figures 8 through 12. Each of these figures clearly indicates that the transmittance of a metallic thin film approaches zero as the thin-film thickness increases. In addition, the reflectance of a metallic thin film approaches a maximum value with increasing thin-film thickness. The maximum value of the reflectance is predicted (Born & Wolf, 1965) by the equation

$$\mathcal{R}_{max} = \frac{n_1^2(1 + \kappa_1^2) + 1 - 2n_1}{n_1^2(1 + \kappa_1^2) + 1 + 2n_1}. \tag{59}$$

The maximum values of the reflectance obtained for the various thin films considered are from equation (59): silver (0.94); aluminum (0.83); gold (0.82); copper (0.73); and iron (0.33).

REGION	THICKNESS (nm)	REFRACTIVE INDEX	ATTENUATION INDEX
LEFT		1.000	0.000
1	300.0	3.500	0.000
RIGHT		1.500	0.000

Incidence Angle: 0.0 (deg)   Wavelength: 500.0 (nm)
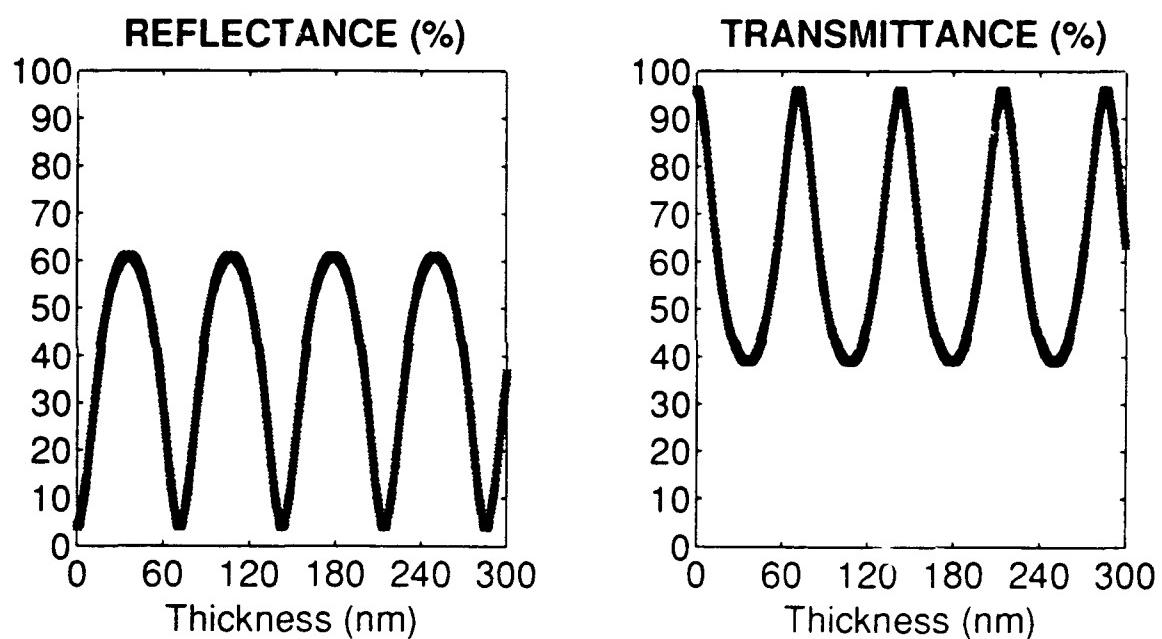
Figure 5. Metallic thin film, attenuation index value of 0.0.

REGION	THICKNESS (nm)	REFRACTIVE INDEX	ATTENUATION INDEX
LEFT		1.000	0.000
1	300.0	3.500	0.100
RIGHT		1.500	0.000

Incidence Angle: 0.0 (deg)   Wavelength: 500.0 (nm)

REFLECTANCE (%)

TRANSMITTANCE (%)
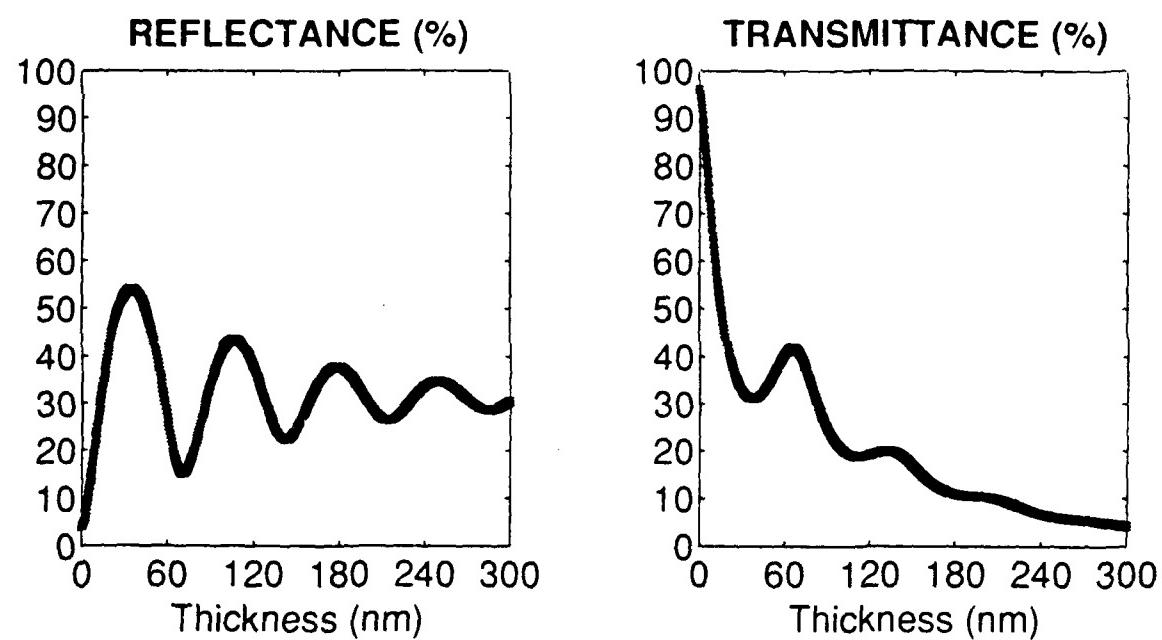
Figure 6. Metallic thin film, attenuation index value of 0.1.

REGION	THICKNESS (nm)	REFRACTIVE INDEX	ATTENUATION INDEX
LEFT		1.000	0.000
1	300.0	3.500	0.200
RIGHT		1.500	0.000

Incidence Angle: 0.0 (deg)   Wavelength: 500.0 (nm)

REFLECTANCE (%)

TRANSMITTANCE (%)

Thickness (nm)   Thickness (nm)
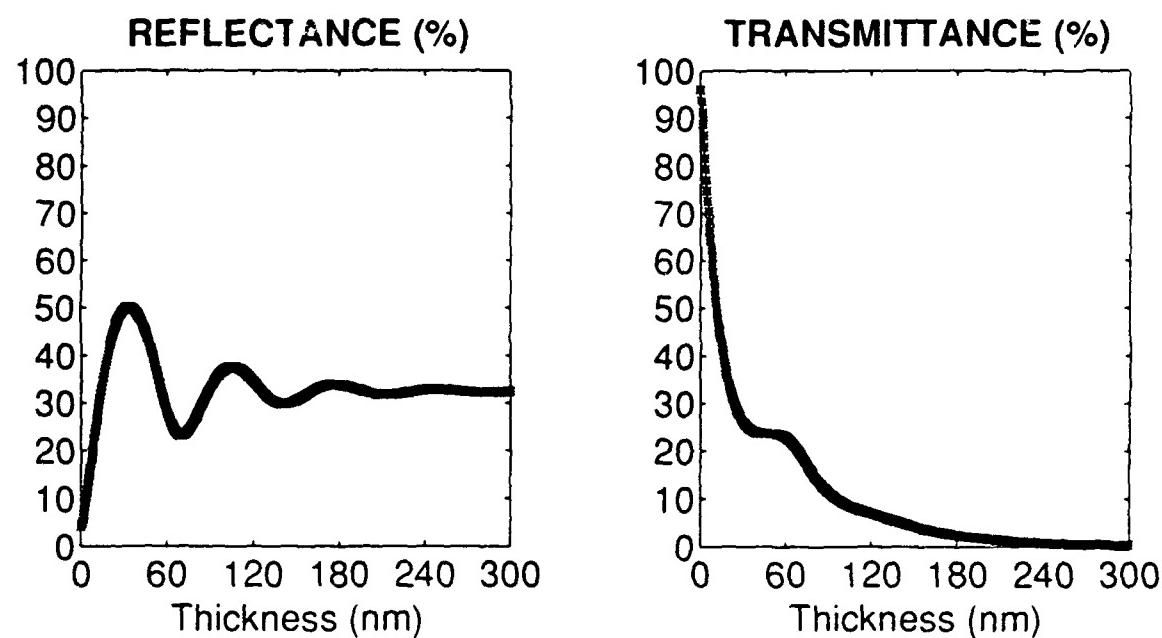
Figure 7. Metallic thin film, attenuation index value of 0.2.

REGION	THICKNESS (nm)	REFRACTIVE INDEX	ATTENUATION INDEX
LEFT		1.000	0.000
1	100.0	0.200	17.200
RIGHT		1.000	0.000

Incidence Angle: 0.0 (deg)   Wavelength: 589.3 (nm)

REFLECTANCE (%)

TRANSMITTANCE (%)
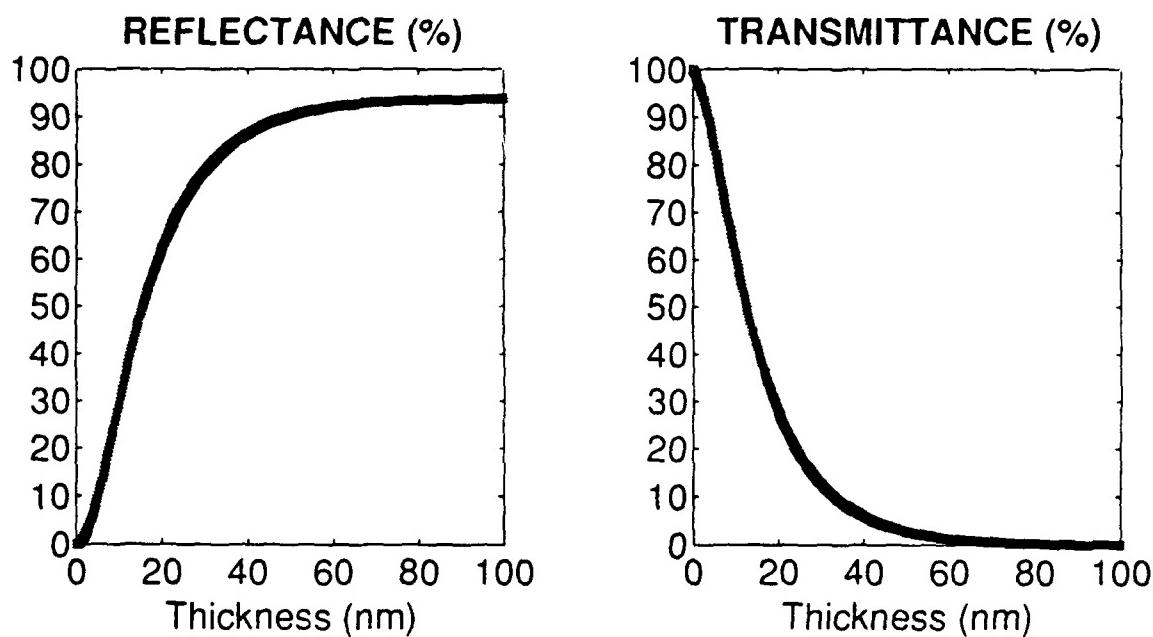
Figure 8. Silver thin film.

REGION	THICKNESS (nm)	REFRACTIVE INDEX	ATTENUATION INDEX
LEFT		1.000	0.000
1	100.0	1.440	3.632
RIGHT		1.000	0.000

Incidence Angle: 0.0 (deg)   Wavelength: 589.3 (nm)
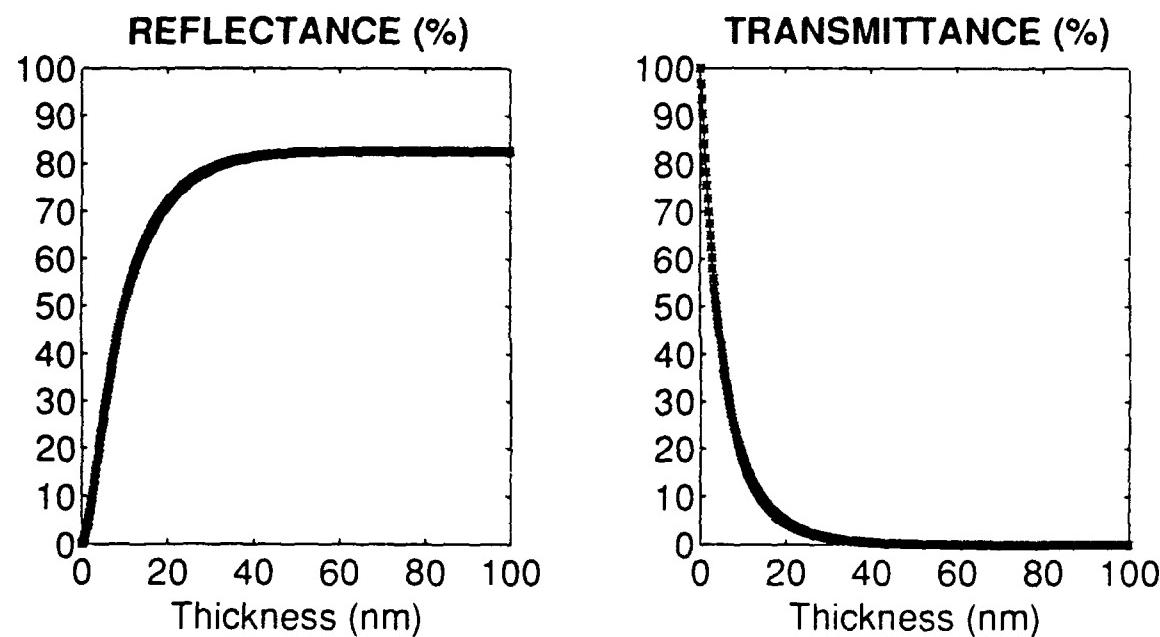
Figure 9. Aluminum thin film.

REGION	THICKNESS (nm)	REFRACTIVE INDEX	ATTENUATION INDEX
LEFT		1.000	0.000
1	100.0	0.470	6.021
RIGHT		1.000	0.000

Incidence Angle: 0.0 (deg)   Wavelength: 589.3 (nm)

REFLECTANCE (%)

TRANSMITTANCE (%)
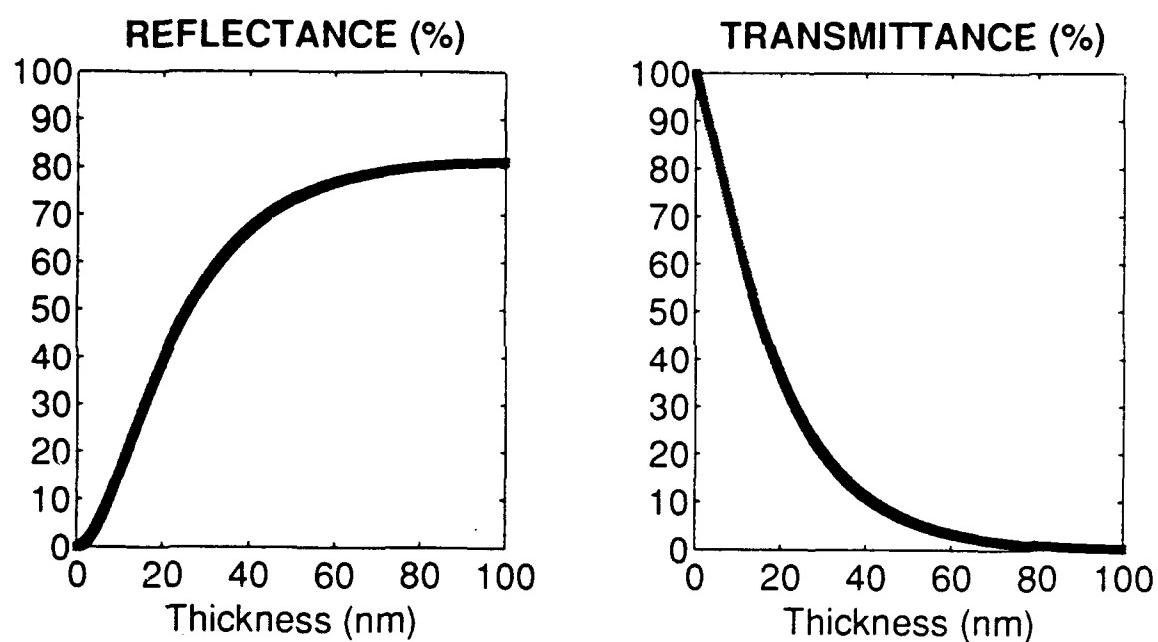
Figure 10. Gold thin film.

REGION	THICKNESS (nm)	REFRACTIVE INDEX	ATTENUATION INDEX
LEFT		1.000	0.000
1	100.0	0.620	4.145
RIGHT		1.000	0.000

Incidence Angle: 0.0 (deg)   Wavelength: 589.3 (nm)
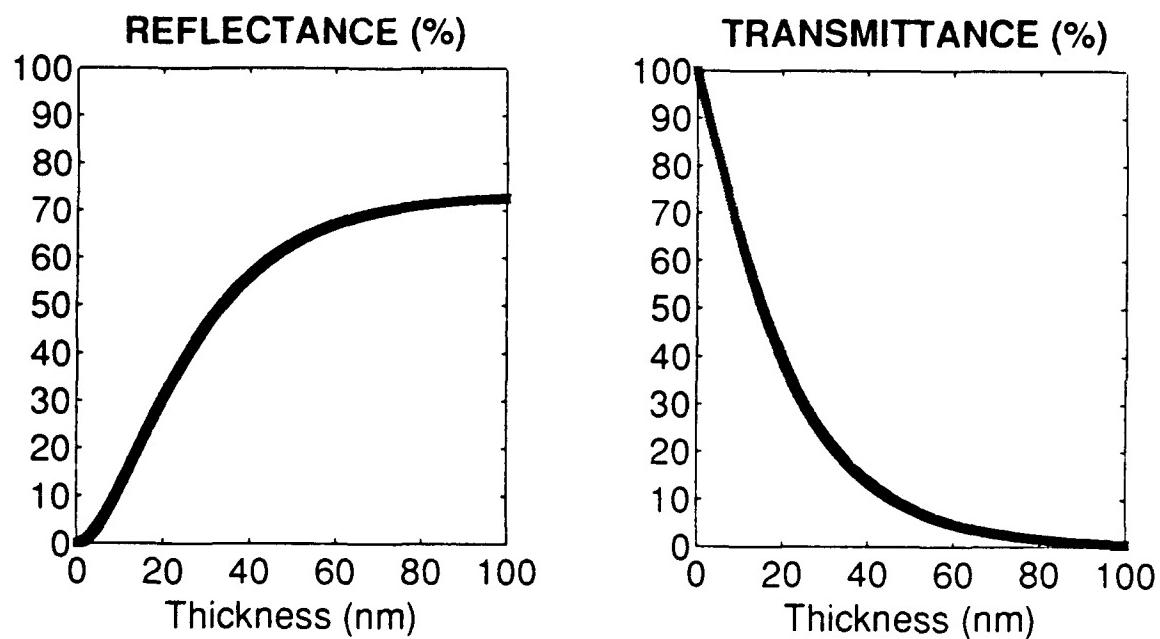
Figure 11. Copper thin film.

REGION	THICKNESS (nm)	REFRACTIVE INDEX	ATTENUATION INDEX
LEFT		1.000	0.000
1	100.0	1.510	1.079
RIGHT		1.000	0.000

Incidence Angle: 0.0 (deg)   Wavelength: 589.3 (nm)

**REFLECTANCE (%)**

TRANSMITTANCE (%)
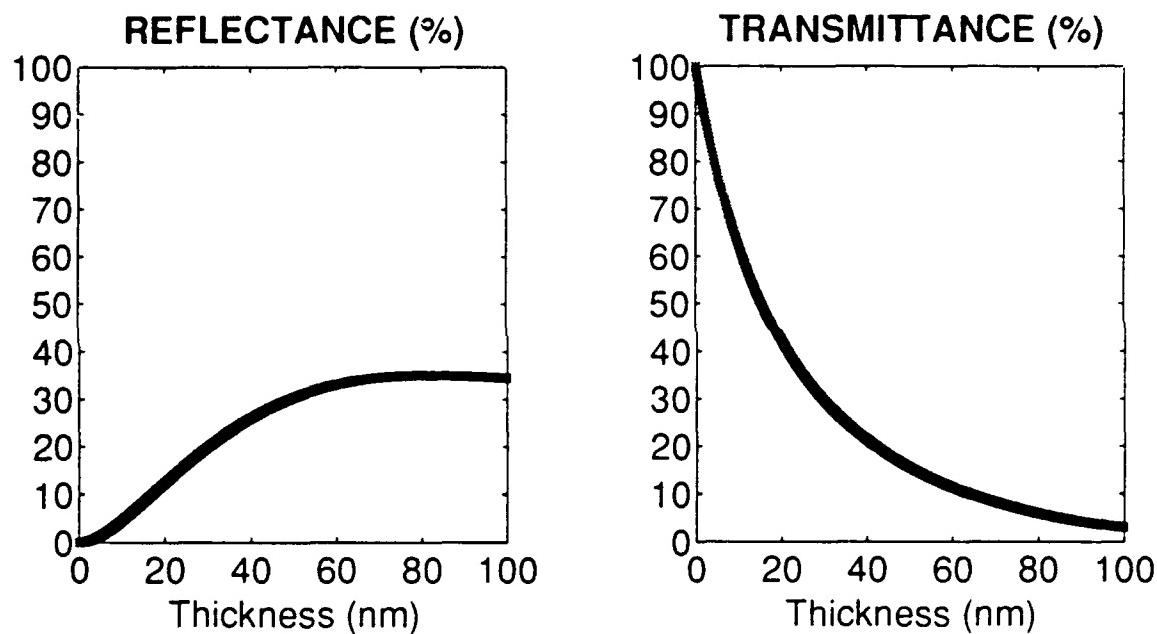
Figure 12. Iron thin film.

3.4 ANTIREFLECTION COATINGS

When an electromagnetic wave impinges upon an optical surface of a prism or lens, a portion of the wave is reflected at the surface. This reflection loss can have deleterious effects on the overall transmission characteristics of the optical device. Reflection losses reduce the overall transmission of optical devices and instruments and often produce unwanted ghost images. The use of antireflection coatings on optical surfaces is a practical method for reducing these undesirable effects. A detailed treatment on the theory of antireflection coatings may be found, for example, in Baumeister (1965), Musset and Thelen (1970), and MacLeod (1986).

We now consider a multilayer optical structure consisting of anywhere from one to four thin-film layers for the purpose of reducing the reflection loss at the interface between two dielectric media. In particular, we will consider the case when the left semi-infinite subregion of space in figure 1 is vacuum and the right semi-infinite subregion is glass with an ordinary refractive index equal to 1.52. The multilayer optical structure is illuminated by a plane-wave at normal incidence. The wavelength was chosen as the variable of interest with values ranging over visible portion of the electromagnetic spectrum from 400 nm (blue) to 700 nm (red). Figures 13 through 16 show the reflectance and transmittance plots obtained when antireflection coatings are employed. The thicknesses and optical properties of the various layers comprising the various multilayer structures considered are summarized in these figures. It is obvious from these figures that the reflection loss at a single surface for normal incidence is approximately 4 percent when the surface is uncoated. Using a single antireflection coating (figure 13) can reduce the losses to approximately 2 percent over the visible spectrum. Two coatings (figure 14) can reduce the reflection losses to approximately 1 percent. Three and four coatings (figures 15 and 16) can further reduce and even eliminate these reflection losses over a substantial portion of the visible spectrum. The MATURE Program computer results presented in figures 13 through 16 are in excellent agreement with results obtained by Musset and Thelen (1970) for the same multilayer structures.

Antireflection coatings can, of course, be used to eliminate unwanted reflections in other portions of the electromagnetic spectrum as well. Figure 17 summarizes the results obtained from the MATLAB 4.0 computer program for wavelengths in the infrared portion of the spectrum for a two-layer antireflection coating. These results are also in excellent agreement with those reported by MacLeod (1986).

REGION	THICKNESS (nm)	REFRACTIVE INDEX	ATTENUATION INDEX
LEFT		1.000	0.000
1	92.4	1.380	0.000
RIGHT		1.520	0.000

Incidence Angle: 0.0 (deg)

REFLECTANCE (%)

Uncoated

Coated

Wavelength (nm)

TRANSMITTANCE (%)

Coated

Uncoated

Wavelength (nm)
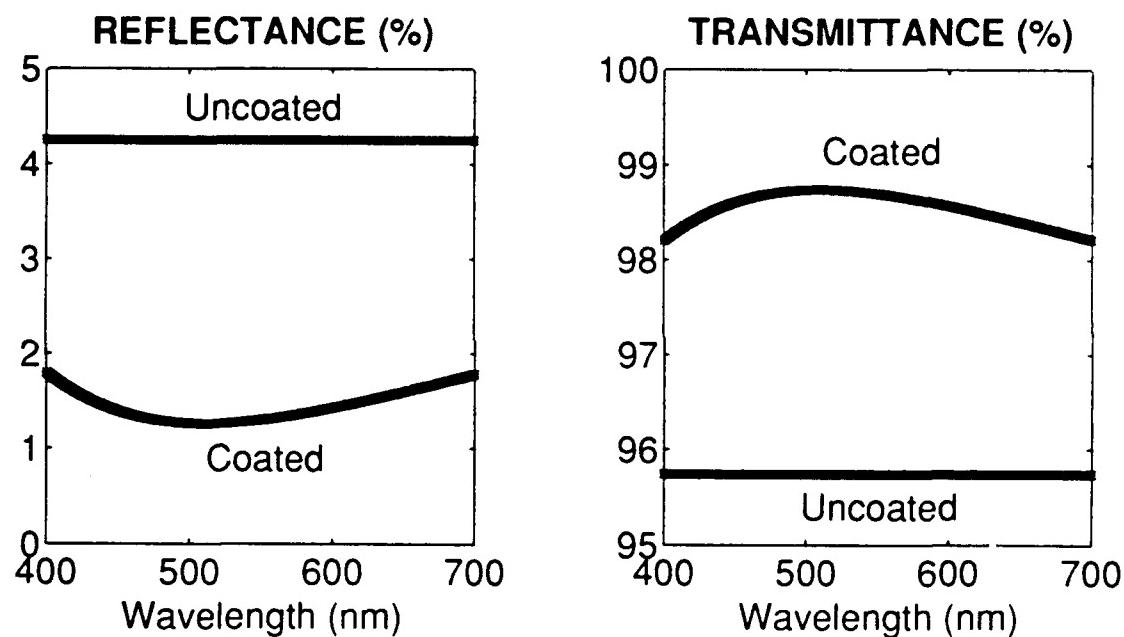
Figure 13. Antireflection coating (1 layer).

REGION	THICKNESS (nm)	REFRACTIVE INDEX	ATTENUATION INDEX
LEFT		1.000	0.000
1	92.4	1.380	0.000
2	159.4	1.600	0.000
RIGHT		1.520	0.000

Incidence Angle: 0.0 (deg)

REFLECTANCE (%)

TRANSMITTANCE (%)
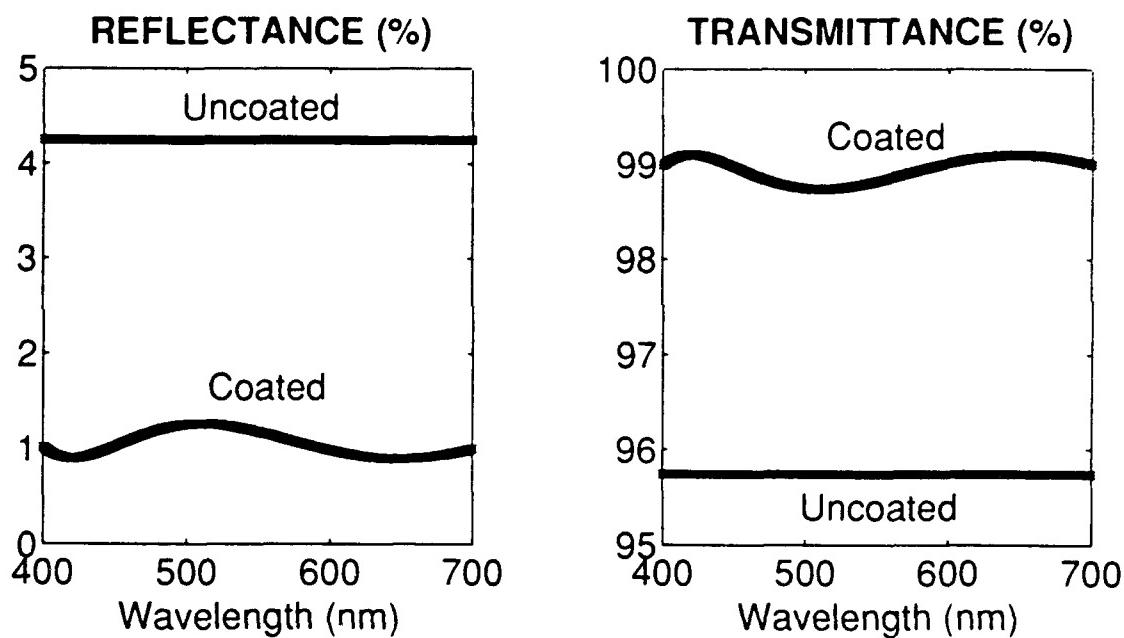
Figure 14. Antireflection coating (2 layers).

REGION	THICKNESS (nm)	REFRACTIVE INDEX	ATTENUATION INDEX
LEFT		1.000	0.000
1	95.1	1.380	0.000
2	122.1	2.150	0.000
3	78.7	1.700	0.000
RIGHT		1.520	0.000

Incidence Angle: 0.0 (deg)
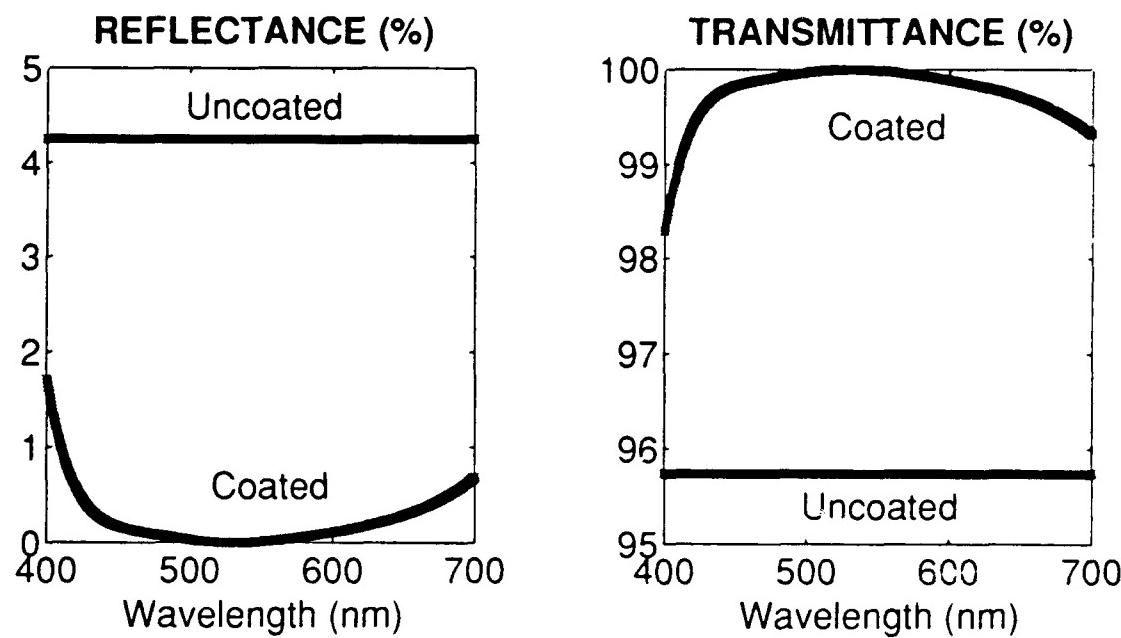
Figure 15. Antireflection coating (3 layers).

REGION	THICKNESS (nm)	REFRACTIVE INDEX	ATTENUATION INDEX
LEFT		1.000	0.000
1	92.1	1.384	0.000
2	108.5	2.350	0.000
3	82.3	1.550	0.000
4	92.1	1.384	0.000
RIGHT		1.520	0.000

Incidence Angle: 0.0 (deg)
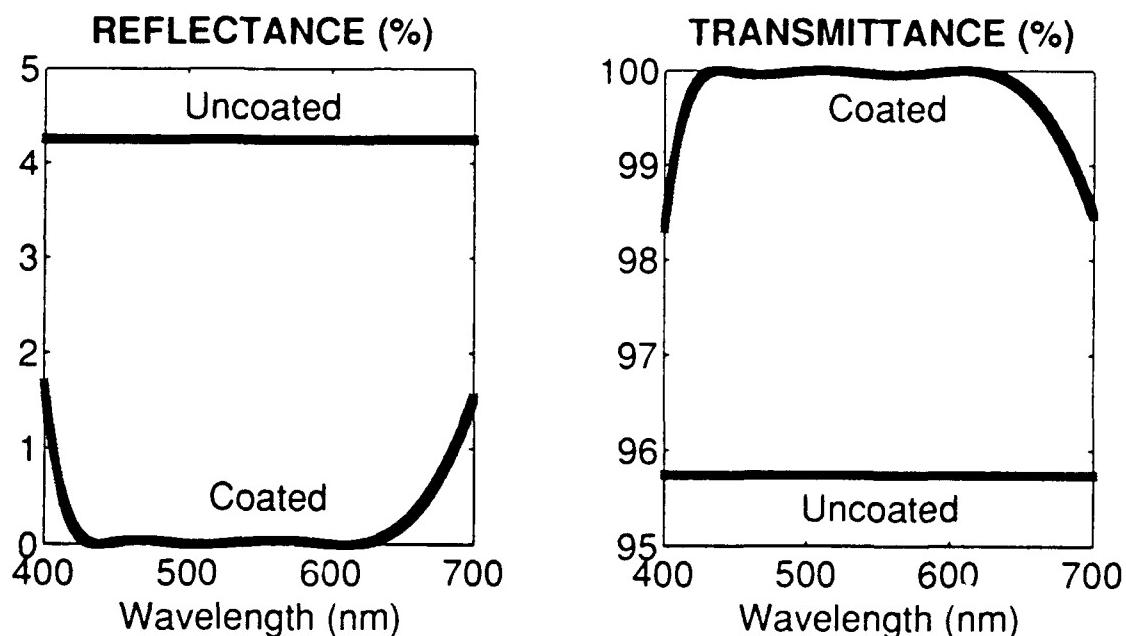
Figure 16. Antireflection coating (4 layers).

REGION	THICKNESS (nm)	REFRACTIVE INDEX	ATTENUATION INDEX
LEFT		1.000	0.000
1	550.3	1.590	0.000
2	347.2	2.520	0.000
RIGHT		4.000	0.000

Incidence Angle: 0.0 (deg)
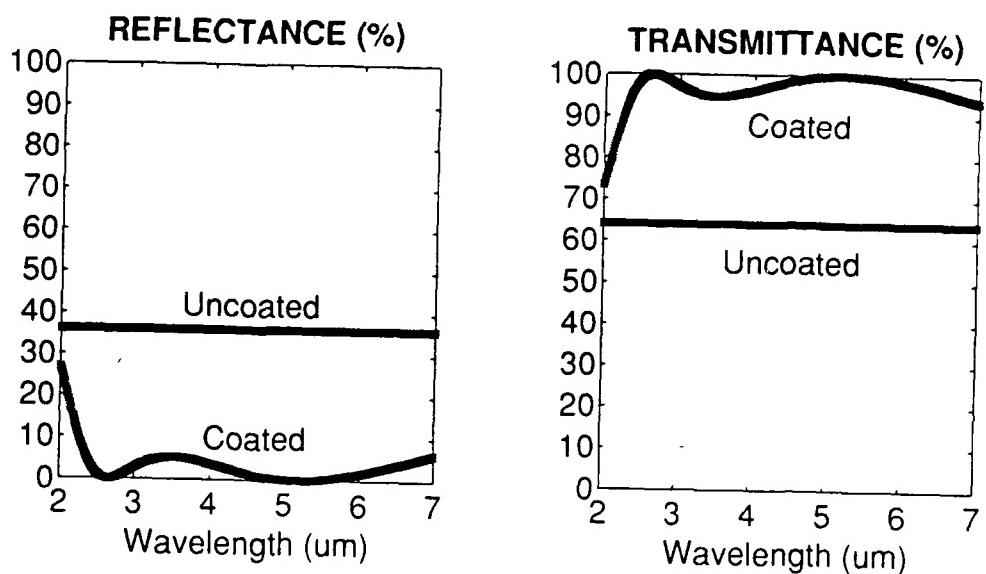
Figure 17. Antireflection coating (IR).

3.5 HIGH-REFLECTANCE COATINGS

Overcoating a glass substrate with a multilayer dielectric thin-film coating is one practical method of fabricating high-reflectance mirrors used in both Fabry-Perot interferometers and laser cavities. Often, these optical devices require mirrors that not only have a reflectance close to 100 percent, but which also transmit a substantial portion of the electromagnetic energy that is not reflected. Metallic thin films of silver, aluminum, or gold seldom attain a reflectance that exceeds 90 percent in the visible portion of the electromagnetic spectrum. However, multilayer dielectric mirrors used for this purpose can attain a reflectance of over 99 percent (Baumeister, 1965).

One type of multilayer dielectric coating used in the fabrication of high-reflectance mirrors is the quarter-wave stack (Baumeister, 1965). Basically, the quarter-wave stack is a multilayer structure where each layer has the same optical thickness, and with refractive indices that alternate between two values. The optical thickness, not to be confused with geometrical thickness of a layer, is simply the product of the refractive index of the layer with its geometrical thickness.

We now consider a multilayer structure having a quarter-wave stack geometry for the purpose of increasing the reflectance at the interface between two dielectric media. Four cases are considered: (1) single-layer; (2) three-layer; (3) five-layer; and (4) a 15-layer stack. We will consider the case when the left semi-infinite subregion of space in figure 1 is vacuum and the right semi-infinite subregion is glass with an ordinary refractive index equal to 1.51. Let the multilayer quarter-wave stack be illuminated by a plane-wave at normal incidence. The wavelength was chosen as the variable of interest. The range of wavelength values varied between 450 nm and 650 nm. Figures 18 through 21 show the reflectance and transmittance plots obtained when high-reflectance coatings are employed. The geometrical thicknesses and optical properties of the various layers comprising the quarter-wave stack considered are summarized in these figures. It is obvious from these figures that the reflectance at a single surface for normal incidence is approximately 4 percent when the surface is uncoated. Using a single high-reflectance coating (figure 18) can increase the reflectance to over 30 percent over the spectral range of interest. Three coatings (figure 19) can increase the reflectance to over 50 percent and five coatings (figure 20) can increase the reflectance to over 70 percent. A 15 layer quarter-wave stack (figure 21) can increase the reflectance to over 99 percent over a substantial portion of the visible spectrum. The results of the MATURE Program presented in figures 18 through 21 are in excellent agreement with results reported by Musset and Thelen (1970) for the same quarter-wave stack structures.

| REGION	THICKNESS (nm)	REFRACTIVE INDEX	ATTENUATION INDEX
LEFT		1.000	0.000
1	57.8	2.300	0.000
RIGHT		1.510	0.000

Incidence Angle: 0.0 (deg)

REFLECTANCE (%)

TRANSMITTANCE (%)
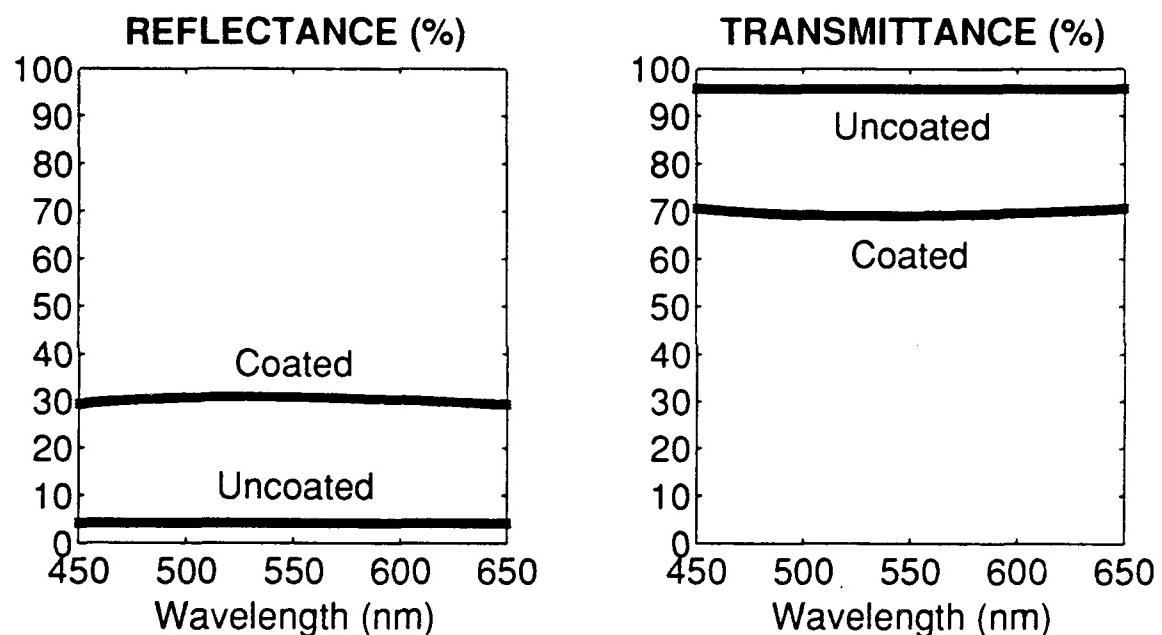
Figure 18. High-reflectance coating (1 layer).

REGION	THICKNESS (nm)	REFRACTIVE INDEX	ATTENUATION INDEX
LEFT		1.000	0.000
1	57.8	2.300	0.000
2	96.4	1.380	0.000
3	57.8	2.300	0.000
RIGHT		1.510	0.000

Incidence Angle: 0.0 (deg)
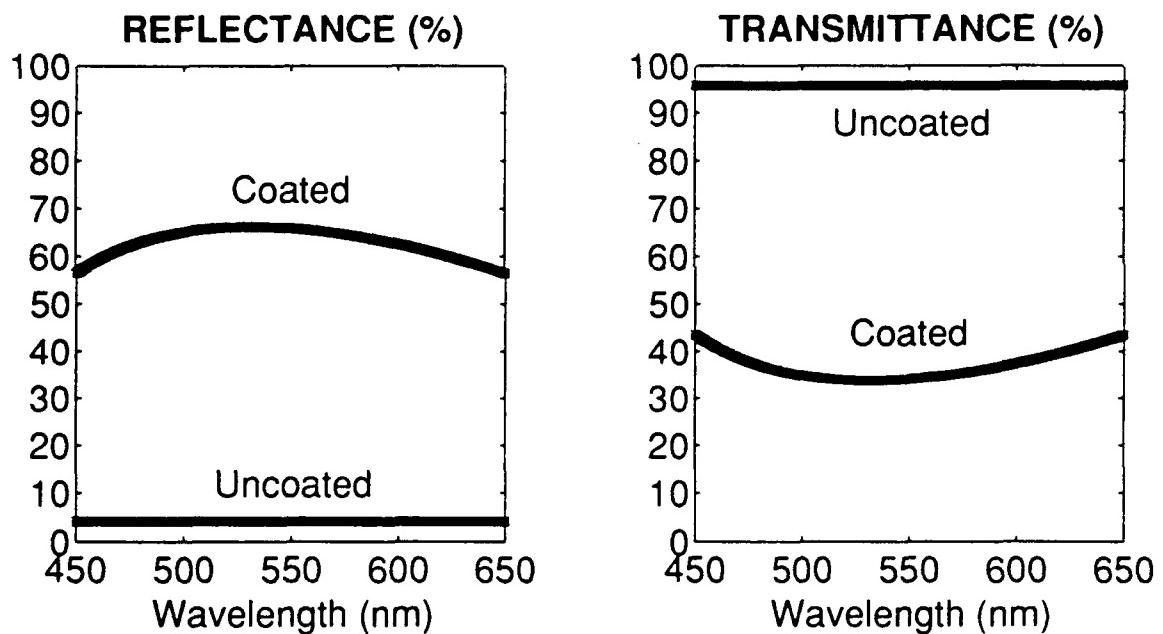
Figure 19. High-reflectance coating (3 layers).

REGION	THICKNESS (nm)	REFRACTIVE INDEX	ATTENUATION INDEX
LEFT		1.000	0.000
1	57.8	2.300	0.000
2	96.4	1.380	0.000
3	57.8	2.300	0.000
4	96.4	1.380	0.000
5	57.8	2.300	0.000
RIGHT		1.510	0.000

Incidence Angle: 0.0 (deg)

REFLECTANCE (%)

Coated

Uncoated

Wavelength (nm)

TRANSMITTANCE (%)

Uncoated

Coated

Wavelength (nm)

Figure 20. High-reflectance coating (5 layers).

| REGION	THICKNESS (nm)	REFRACTIVE INDEX	ATTENUATION INDEX
LEFT		1.000	0.000
1	57.8	2.300	0.000
2	96.4	1.380	0.000
3	57.8	2.300	0.000
4	96.4	1.380	0.000
5	57.8	2.300	0.000
6	96.4	1.380	0.000
7	57.8	2.300	0.000
8	96.4	1.380	0.000
9	57.8	2.300	0.000
10	96.4	1.380	0.000
11	57.8	2.300	0.000
12	96.4	1.380	0.000
13	57.8	2.300	0.000
14	96.4	1.380	0.000
15	57.8	2.300	0.000
RIGHT		1.510	0.000

Incidence Angle: 0.0 (deg)
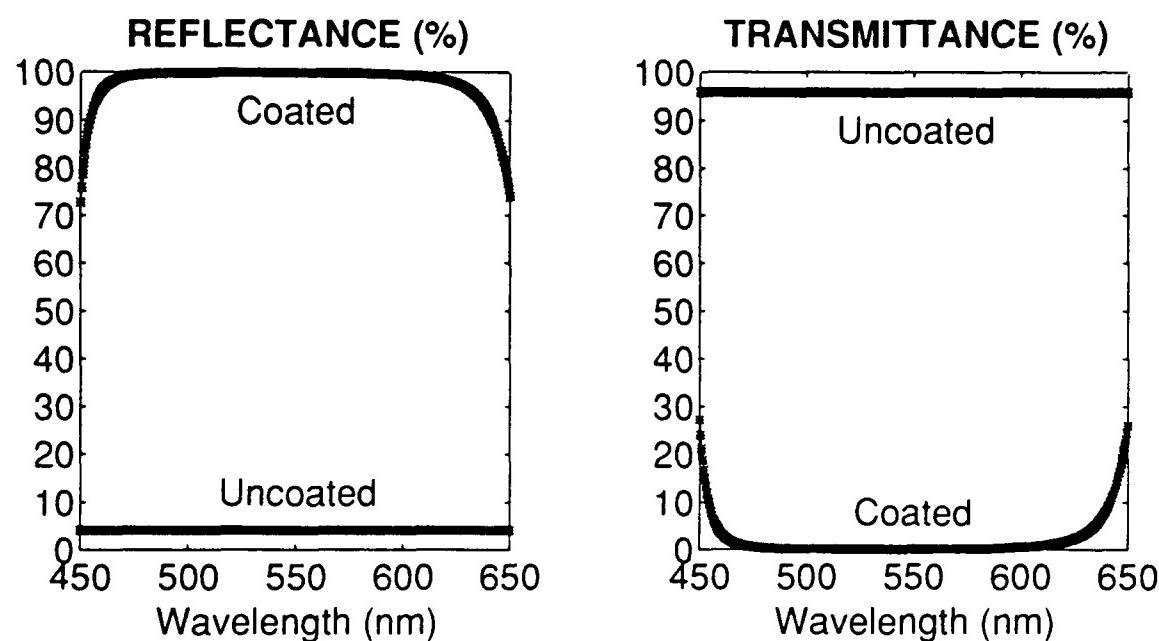
Figure 21. High-reflectance coating (15 layers).

3.6 MULTILAYER INTERFERENCE BAND-PASS FILTER

Multilayer interference band-pass filters are often used in place of a prism or diffraction grating in spectrophotometric systems. These filters, for a given resolving power, are the most luminous instrument available. The advantage of using only dielectric films, as opposed to metallic films, is that the peak transmittance is high and a narrowband pass can be achieved. A detailed discussion on the fabrication and use of multilayer interference filters can be found in Hernandez (1986).

The quarter-wave stack previously mentioned in our discussion on high-reflectance coatings also finds use in the fabrication of multilayer interference band-pass filters. One geometry involves sandwiching a half-wave spacer between two identical quarter-wave stacks (Baumeister, 1965). We now consider a multilayer structure having this geometry. Three cases are considered: (1) a 7-layer; (2) an 11-layer; and (3) a 15-layer filter. We consider the scenario for which the left semi-infinite subregion of space in figure 1 is vacuum and the right semi-infinite subregion is glass with an ordinary refractive index equal to 1.51. Let the multilayer filter be illuminated by a plane-wave whose wavelength is varied between 500 nm and 600 nm. Shown in figures 22 through 24 are reflectance and transmittance plots obtained for the 7-layer, 11-layer, and 15-layer filters respectively for the case of normal incidence. The geometrical thicknesses and optical properties of the layers comprising these various multilayer filters are also summarized in these figures. It is obvious from these figures that the band pass of an interference filter decreases as the number of layers in each of the quarter-wave stacks increases. Shown next in figures 25 and 26 is the effect angle of incidence has on the reflectance and transmittance characteristics of an 11-layer interference filter. Plots for angles of incidence equal to 0°, 30°, and 45° are shown. The results presented in figure 25 are for an incident wave having a TE polarization state, whereas those in figure 26 correspond to an incident wave having a TM polarization state. It is obvious from these figures how the band pass of the interference filter is shifted to shorter wavelengths as the angle of incidence is increased. We see that the interference filter characteristics also depend on the polarization state of the incident plane-wave.

Shown in figure 27 are reflectance and transmittance plots obtained using the MATURE Program of a three-layer Fabry-Perot etalon where two identical silver thin films are used in conjunction with a single dielectric spacer. Notice, as a result of absorption within the metallic films of the etalon, how the overall transmittance of the etalon is greatly reduced in comparison to that of an all-dielectric interference filter. This demonstrates the advantage of using only dielectric thin films in interference filters.

41

| REGION	THICKNESS (nm)	REFRACTIVE INDEX	ATTENUATION INDEX
LEFT		1.000	0.000
1	59.8	2.300	0.000
2	99.6	1.380	0.000
3	59.8	2.300	0.000
4	199.3	1.380	0.000
5	59.8	2.300	0.000
6	99.6	1.380	0.000
7	59.8	2.300	0.000
RIGHT		1.510	0.000

Incidence Angle: 0.0 (deg)
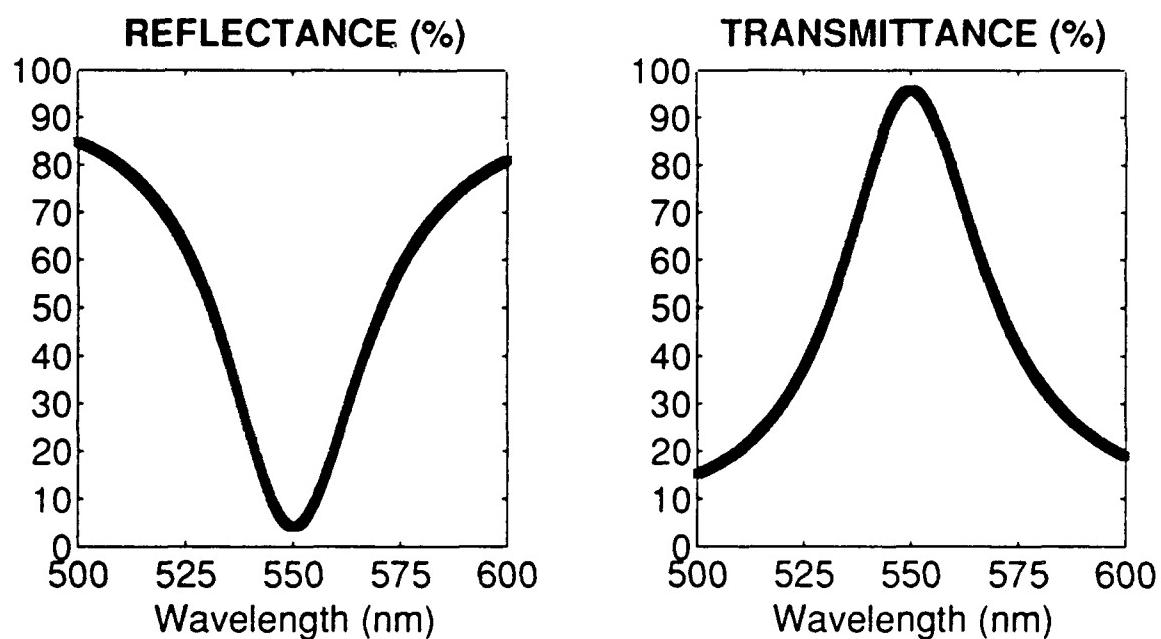
Figure 22. Band-pass filter (7 layers).

| REGION	THICKNESS (nm)	REFRACTIVE INDEX	ATTENUATION INDEX
LEFT		1.000	0.000
1	59.8	2.300	0.000
2	99.6	1.380	0.000
3	59.8	2.300	0.000
4	99.6	1.380	0.000
5	59.8	2.300	0.000
6	199.3	1.380	0.000
7	59.8	2.300	0.000
8	99.6	1.380	0.000
9	59.8	2.300	0.000
10	99.6	1.380	0.000
11	59.8	2.300	0.000
RIGHT		1.510	0.000

Incidence Angle: 0.0 (deg)

Figure 23. Band-pass filter (11 layers).

REGION	THICKNESS (nm)	REFRACTIVE INDEX	ATTENUATION INDEX
LEFT		1.000	0.000
1	59.8	2.300	0.000
2	99.6	1.380	0.000
3	59.8	2.300	0.000
4	99.6	1.380	0.000
5	59.8	2.300	0.000
6	99.6	1.380	0.000
7	59.8	2.300	0.000
8	199.3	1.380	0.000
9	59.8	2.300	0.000
10	99.6	1.380	0.000
11	59.8	2.300	0.000
12	99.6	1.380	0.000
13	59.8	2.300	0.000
14	99.6	1.380	0.000
15	59.8	2.300	0.000
RIGHT		1.510	0.000

Incidence Angle: 0.0 (deg)
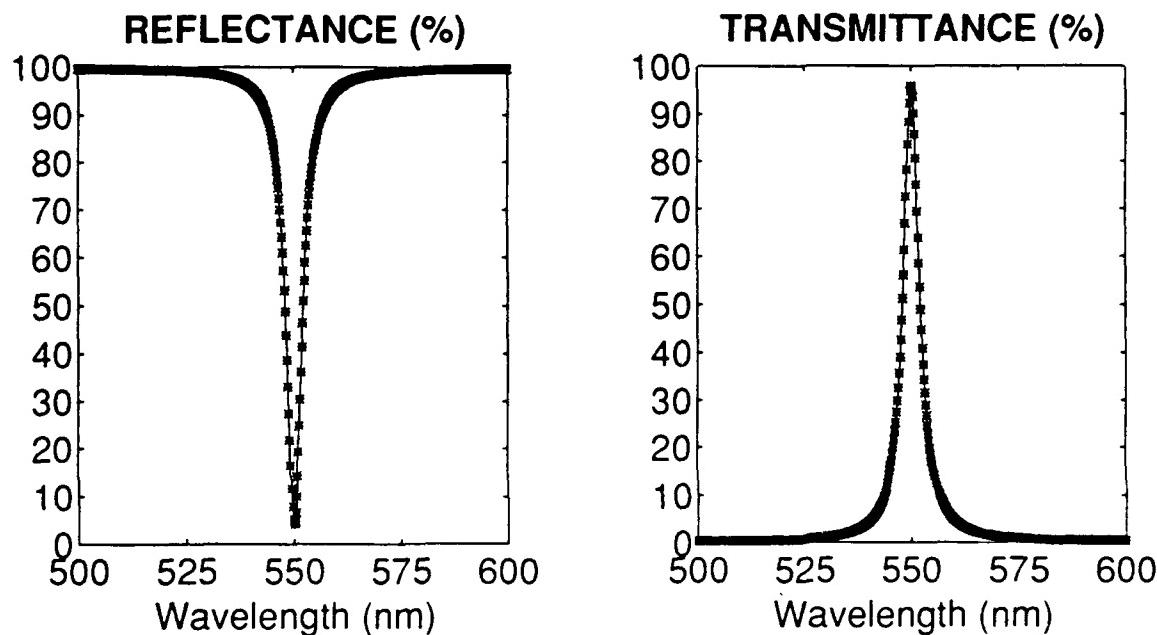
Figure 24. Band-pass filter (15 layers).

REGION	THICKNESS (nm)	REFRACTIVE INDEX	ATTENUATION INDEX
LEFT		1.000	0.000
1	59.8	2.300	0.000
2	99.6	1.380	0.000
3	59.8	2.300	0.000
4	99.6	1.380	0.000
5	59.8	2.300	0.000
6	199.3	1.380	0.000
7	59.8	2.300	0.000
8	99.6	1.380	0.000
9	59.8	2.300	0.000
10	99.6	1.380	0.000
11	59.8	2.300	0.000
RIGHT		1.510	0.000

Incidence Angle: 0, 30, 45 (deg)

Figure 25. Band-pass filter (11 layers, TE polarization).

REGION	THICKNESS (nm)	REFRACTIVE INDEX	ATTENUATION INDEX
LEFT		1.000	0.000
1	59.8	2.300	0.000
2	99.6	1.380	0.000
3	59.8	2.300	0.000
4	99.6	1.380	0.000
5	59.8	2.300	0.000
6	199.3	1.380	0.000
7	59.8	2.300	0.000
8	99.6	1.380	0.000
9	59.8	2.300	0.000
10	99.6	1.380	0.000
11	59.8	2.300	0.000
RIGHT		1.510	0.000

Incidence Angle: 0, 30, 45 (deg)

Figure 26. Band-pass filter (11 layers, TM polarization).

REGION	THICKNESS (nm)	REFRACTIVE INDEX	ATTENUATION INDEX
LEFT		1.000	0.000
1	34.0	0.200	17.200
2	340.0	1.380	0.000
3	34.0	0.200	17.200
RIGHT		1.510	0.000

Incidence Angle: 0.0 (deg)
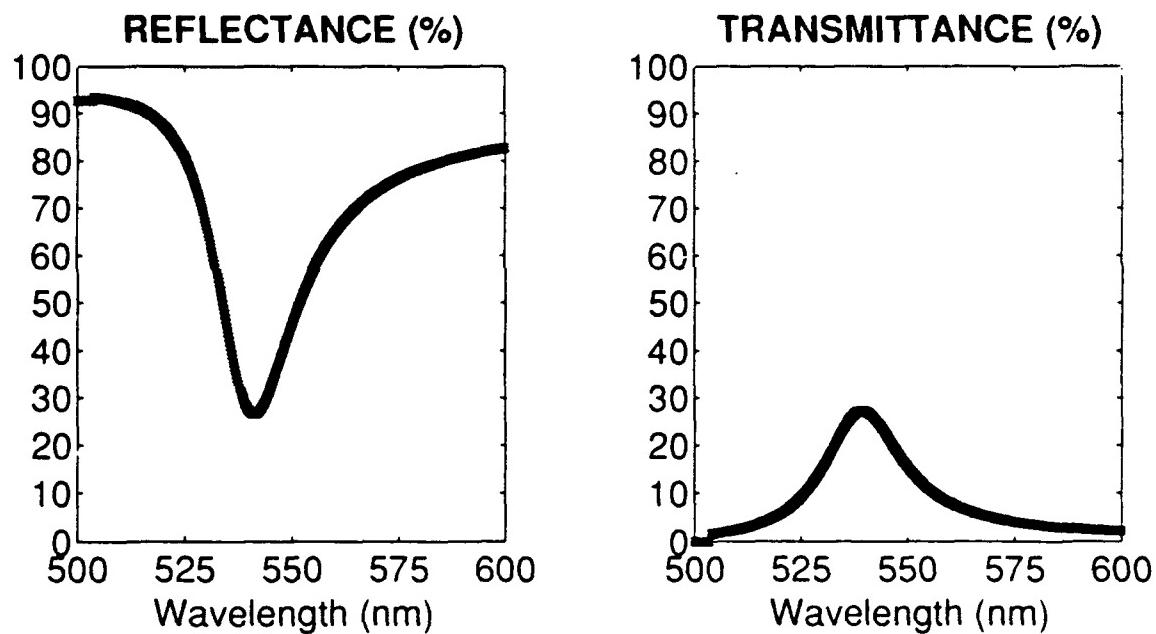
Figure 27. Fabry-Perot etalon with silver mirrors.

4.0 SUMMARY AND CONCLUSIONS

Presented in this publication is a new approach, based entirely on the use of matrices, for solving electromagnetic wave propagation problems involving multilayer dielectric media with planar boundaries. This new approach is based upon a reformulation of the traditional vector form of the Maxwell field equations into a single matrix equation containing square 8 by 8 differential matrix operators. Boundary conditions are taken into account by partitioning both the electromagnetic wavefunctions and the dielectric, permeability, and conductivity matrices describing the optical medium using combinations of Heaviside step functions called partition functions. Using monochromatic plane-wave representations of the electromagnetic field, we were able to develop an 8 by 8 system operator description of wave propagation through the entire multilayer medium. This operator description led to a set of equations for predicting both the reflection and transmission characteristics of a multilayer medium with planar boundaries illuminated by a monochromatic plane-wave electromagnetic radiation.

Because of the power of matrix operations, many of the fundamental relationships and results in electromagnetic wave propagation theory are easily derived without the need for the usual plethora of vector calculus identities that have become the standard in these derivations: Stokes' theorem, the Divergence theorem, the formula for the curl of a curl, etc. Instead, mathematical operations involving matrix multiplication, matrix inversion, and eigensolutions of matrices can be employed. Readily available off-the-shelf computer software packages, like MATLAB for numerical computations and MATHEMATICA for symbolic manipulations, are well suited for these matrix operations. A computer software package entitled MATURE is currently being written and tested at NRaD to handle a variety of scenarios involving electromagnetic wave propagation. MATURE is the acronym for Matrix Approach To Understanding Relativistic Electrodynamics. The MATURE computer software program is being written using MATLAB code for use on a Sun 4 SPARCstation 2 workstation.

With the present version of the MATURE Program, several numerical examples were considered that illustrate the power and utility of using the 8 by 8 matrix representation in solving wave propagation problems. Examples considered included: (1) reflection and refraction at a single interface separating two dielectric media, (2) evanescent wave coupling from one dielectric medium into another via a vacuous thin film, (3) the reflection and transmission properties of a single conducting thin metallic film, (4) the reflection and transmission characteristics of a multilayer antireflection coating structure, (5) the reflection and transmission properties of a multilayer high-reflectance mirror, and (6) the reflection and transmission characteristics of a multilayer interference band-pass filter. The MATURE Program is quite general in that the reflection and transmission characteristics of the multilayer medium can be determined for arbitrarily chosen wavelengths, angles of incidence, and polarization states of the incident electromagnetic radiation.

REFERENCES

Baumeister, P. 1965. *Interference, and Optical Interference Coatings*, in Applied Optics and Optical Engineering, Vol. I, R. Kingslake, editor, Academic Press, New York, NY.

Bocker, R. P., and B. R. Frieden. 1992. "A New Matrix Formulation of Classical Electrodynamics. Part I. Vacuum." TD 2259. Naval Command, Control, and Ocean Surveillance Center, RDT&E Division, San Diego, CA.

Bocker, R. P. 1992. "A New Matrix Formulation of Classical Electrodynamics. Part II. Wave Propagation in Optical Materials of Infinite Extent." TD 2320. Naval Command, Control, and Ocean Surveillance Center, RDTE Division, San Diego, CA.

Born, M., and E. Wolf. 1965. *Principles of Optics*, Pergamon Press, Oxford, England.

Bracewell, R. 1965. *The Fourier Transform and Its Applications*, McGraw-Hill Book Company, New York, NY.

Fowles, G. R. 1968. *Introduction to Modern Optics*, Holt, Rinehart, and Winston, Inc., New York, NY.

Hernandez, G. 1986. *Fabry-Perot Interferometers*, Cambridge University Press, Cambridge, England.

Jackson, J. D. 1962. *Classical Electrodynamics*, John Wiley and Sons, Inc., New York, NY.

MacLeod, H. A. 1986. *Thin-Film Optical Filters*, McGraw-Hill, Inc., New York, NY.

Magid, L. M. 1972. *Electromagnetic Fields, Energy, and Waves*, John Wiley and Sons, Inc., New York, NY.

Musset, A., and A. Thelen. 1970. *Multilayer Antireflection Coatings*, in Progress on Optics, Vol. VIII, E. Wolf, editor, North-Holland Publishing Company, Amsterdam.

Wylie, C. R. 1953. *Calculus*, McGraw-Hill Book Company, Inc., New York, NY.

APPENDIX A

PARTITION FUNCTIONS

The partition functions, first introduced in section 2.3 of this report, are defined in this appendix. Recall that the multilayer optical medium depicted in figure 1 consists of a finite number, N, of planar layers each having a finite thickness as measured along the z-direction. All layer interfaces are parallel as well as being orthogonal to the z-axis. Each of these layers is labelled by an integer, n, where $n = 1, 2, ..., N$. To the left of the multilayer medium is a semi-infinite subregion of space denoted by the label 0. And to the right of the multilayer medium is a second semi-infinite subregion of space denoted by the label $N+1$. Associated with each of the layers comprising the multilayer medium and the two semi-infinite subregions of space is a partition function. These partition functions are defined by equations (A.1) through (A.3) below. Those properties of the partition functions pertinent to this investigation are contained in equations (A.4) through (A.8). It is noted that the partition functions are simply Heaviside unit step functions (Bracewell, 1965) or linear combinations thereof.

The partition function associated with the semi-infinite subregion of space labelled 0 is defined by the following equation

$$\Psi_0(z) \equiv \begin{cases} 1 & z < z_0 \\ 0 & otherwise. \end{cases} \tag{A.1}$$

Associated with each layer, n, of the multilayer optical medium is a partition function defined by

$$\Psi_n(z) \equiv \begin{cases} 1 & z_{n-1} < z < z_n \\ 0 & otherwise \end{cases} \qquad (n = 1, 2, 3, ..., N) \tag{A.2}$$

The semi-infinite subregion of space labelled $N+1$ is represented by a partition function defined by

$$\Psi_{N+1}(z) \equiv \begin{cases} 1 & z_N < z \\ 0 & otherwise. \end{cases} \tag{A.3}$$

All of the partition functions defined above satisfy the following property

$$\Psi_m(z)\Psi_n(z) = \delta_{mn}\Psi_n(z) \tag{A.4}$$

where δ_{mn} is the Kronecker delta (Bracewell, 1965). Each partition function $\Psi_n(z)$ has a first derivative with respect to the variable z, denoted by the function $\Phi_n(z)$. Mathematically

$$\Phi_n(z) \equiv \frac{d}{dz}\Psi_n(z) \qquad (n = 0, 1, 2, 3, ..., N, N+1). \tag{A.5}$$

Using the fact that the first derivative of the Heaviside unit step is the Dirac delta function (Bracewell, 1965), it can be easily shown that

$$\Phi_0(z) = -\delta(z - z_0) \tag{A.6}$$

$$\Phi_n(z) = +\delta(z - z_{n-1}) - \delta(z - z_n) \qquad (n = 1, 2, 3, ..., N) \tag{A.7}$$

$$\Phi_{N+1}(z) = +\delta(z - z_N) \tag{A.8}$$

where $\delta(z)$ represents the Dirac delta function.

REFERENCE

Bracewell, R. 1965. *The Fourier Transform and Its Applications*, McGraw-Hill Book Company, New York, NY.

APPENDIX B

ELECTROMAGNETIC PLANE-WAVE SOLUTIONS

Monochromatic electromagnetic plane-wave solutions satisfying the Maxwell field equations are of vital importance to our understanding of wave propagation through a multilayer optical medium. We start with the matrix representation of the Maxwell field equations for an unbounded dielectric medium as summarized by equation (19) and rewritten here in equation (B.1) for convenience.

$$
\begin{bmatrix} M_1\varepsilon + i\gamma & M_2 \\ M_2 & M_1\mu \end{bmatrix} \begin{bmatrix} f_1 \\ f_2 \end{bmatrix} = \begin{bmatrix} 0 \\ 0 \end{bmatrix}. \tag{B.1}
$$

For monochromatic electromagnetic plane-wave fields, the electromagnetic field vector appearing in equation (B.1) can be expressed in the form

$$
\begin{bmatrix} f_1 \\ f_2 \end{bmatrix} = \begin{bmatrix} f_{01} \\ f_{02} \end{bmatrix} exp\{i[r]^T[k]\}. \tag{B.2}
$$

The 4 by 1 vectors $[f_{01}]$ and $[f_{02}]$ are both constant and describe the polarization properties of the plane-wave field. With the use of equation (10), they can be expressed in the form

$$
[f_{01}] = i\begin{bmatrix} E_{ox} \\ E_{oy} \\ E_{oz} \\ 0 \end{bmatrix} \quad and \quad [f_{02}] = \begin{bmatrix} H_{ox} \\ H_{oy} \\ H_{oz} \\ 0 \end{bmatrix}. \tag{B.3}
$$

The relativistic 4-vectors $[r]$ and $[k]$ appearing in equation (B.2) are defined by

$$
[r] \equiv \begin{bmatrix} x \\ y \\ z \\ \tau \end{bmatrix} \quad and \quad [k] \equiv \begin{bmatrix} k_x \\ k_y \\ k_z \\ k_\tau \end{bmatrix} \tag{B.4}
$$

where

$$\tau = ict \quad and \quad k_\tau = \frac{i\omega}{c}. \tag{B.5}$$

Again, the imaginary unit i is equal to $\sqrt{-1}$ and c represents the speed of light in vacuum. The quantity ω represents the angular frequency of the monochromatic plane-wave. The superscript, T, appearing in equation (B.2) denotes transpose. The dot (scalar) product of the vectors $[r]$ and $[k]$ is given by

$$[r]^T [k] = xk_x + yk_y + zk_z - \omega t = k \bullet r - \omega t. \tag{B.6}$$

The three-dimensional wave vector k above can be expressed in the form

$$k = (k_x, k_y, k_z) = k(\alpha_x, \alpha_y, \alpha_z) = k\hat{\alpha} \tag{B.7}$$

where the scalar k is the wavenumber. The unit vector $\hat{\alpha}$ has as its components the direction cosines $\alpha_x, \alpha_y, \alpha_z$, which satisfy the equation (Morrill, 1961)

$$\alpha_x^2 + \alpha_y^2 + \alpha_z^2 = 1. \tag{B.8}$$

Next we define two direction cosine matrices $[\alpha_1]$ and $[\alpha_2]$ by the equation

$$[\alpha_1] \equiv \begin{bmatrix} 0 & 0 & 0 & -\alpha_x \\ 0 & 0 & 0 & -\alpha_y \\ 0 & 0 & 0 & -\alpha_z \\ +\alpha_x & +\alpha_y & +\alpha_z & 0 \end{bmatrix} \quad and \quad [\alpha_2] \equiv \begin{bmatrix} 0 & -\alpha_z & +\alpha_y & 0 \\ +\alpha_z & 0 & -\alpha_x & 0 \\ -\alpha_y & +\alpha_x & 0 & 0 \\ 0 & 0 & 0 & 0 \end{bmatrix}. \tag{B.9}$$

Recall that the 4 by 4 matrix $[\gamma]$ appearing in equation (B.1) is defined in terms of the conductivity tensor $[\sigma]$ by equation (20), which has been rewritten in equation (B.10) below for convenience.

$$[\gamma] = \frac{4\pi}{c} [\sigma]. \tag{B.10}$$

The complex dielectric tensor $[\hat{\varepsilon}]$ (Born and Wolf, 1965) is defined in terms of the dielectric tensor $[\varepsilon]$ and the conductivity tensor $[\sigma]$ by the equation

$$[\hat{\varepsilon}] \equiv [\varepsilon] + i\frac{4\pi}{\omega} [\sigma]. \tag{B.11}$$

It can be easily shown that substitution of the electromagnetic plane-wave solution (B.2) back into the Maxwell field equations (B.1) gives the following matrix equation

$$\begin{bmatrix} \alpha_1 \varepsilon & \alpha_2 \\ \alpha_2 & \alpha_1 \mu \end{bmatrix} \begin{bmatrix} f_{01} \\ f_{02} \end{bmatrix} = \frac{i\omega}{kc} \begin{bmatrix} \hat{\varepsilon} & 0 \\ 0 & \mu \end{bmatrix} \begin{bmatrix} f_{01} \\ f_{02} \end{bmatrix}. \tag{B.12}$$

By performing the matrix multiplication operations suggested in equation (B.12), it can be easily verified that

$$[\alpha_1] [f_{01}] = [o] \qquad and \qquad [\alpha_1] [f_{02}] = [o] \tag{B.13}$$

and

$$[\alpha_2] [f_{01}] = \mu \frac{i\omega}{kc} [f_{02}] \qquad and \qquad [\alpha_2] [f_{02}] = \hat{\varepsilon} \frac{i\omega}{kc} [f_{01}] . \tag{B.14}$$

Equations (B.13) and (B.14) can be combined to form

$$[\alpha_1 + \alpha_2] [f_{01}] = \mu \frac{i\omega}{kc} [f_{02}] \qquad and \qquad [\alpha_1 + \alpha_2] [f_{02}] = \hat{\varepsilon} \frac{i\omega}{kc} [f_{01}] , \tag{B.15}$$

which has numerical stability attributes not found in equation (B.14) under the operation of matrix inversion. It can be easily shown that the sum of the direction cosine matrices has the property

$$[\alpha_1 + \alpha_2] [\alpha_1 + \alpha_2] = -[I] \tag{B.16}$$

where $[I]$ is the 4 by 4 identity matrix. This implies that $[\alpha_1 + \alpha_2]$ has a multiplicative inverse given by

$$[\alpha_1 + \alpha_2]^{-1} = -[\alpha_1 + \alpha_2] . \tag{B.17}$$

Multiplying either equation in (B.15) by the matrix $[\alpha_1 + \alpha_2]$ and using the remaining equation in (B.15) with the multiplicative property (B.16) gives

$$\frac{\omega^2 \mu \hat{\varepsilon}}{k^2 c^2} = 1 . \tag{B.18}$$

From this equation we obtain the following expression for the wavenumber k

$$k = \frac{\omega}{c} \sqrt{\mu \hat{\varepsilon}} \tag{B.19}$$

which we see is complex for a conductive medium. With the use of equation (B.19), equation (B.15) can be rewritten in the finalized symmetrical form

$$[f_{01}] = -i\sqrt{\frac{\mu}{\hat{\varepsilon}}}\,[\alpha_1 + \alpha_2]\,[f_{02}] \qquad and \qquad [f_{02}] = -i\sqrt{\frac{\hat{\varepsilon}}{\mu}}\,[\alpha_1 + \alpha_2]\,[f_{01}]. \qquad (B.20)$$

For completeness, equation (B.20) is equivalent to the following vector equations

$$\hat{\alpha} \bullet E_o = 0 \qquad and \qquad \hat{\alpha} \bullet H_o = 0 \qquad (B.21)$$

$$E_o = -\sqrt{\frac{\mu}{\hat{\varepsilon}}}\,(\hat{\alpha} \times H_o) \qquad and \qquad H_o = +\sqrt{\frac{\hat{\varepsilon}}{\mu}}\,(\hat{\alpha} \times E_o) \qquad (B.22)$$

where

$$E_o \equiv (E_{ox}, E_{oy}, E_{oz}) \qquad and \qquad H_o \equiv (H_{ox}, H_{oy}, H_{oz}). \qquad (B.23)$$

Equations (B.21) and (B.22), and hence equation (B.20), express the transversal nature of the electric and magnetic fields associated with the monochromatic electromagnetic plane-wave solutions (B.2).

It is of interest to note that the complex index of refraction (Born and Wolf, 1965) is given by the equation

$$\hat{n} = \sqrt{\mu\hat{\varepsilon}}. \qquad (B.24)$$

In addition, the complex index of refraction can also be written in the following form (Born and Wolf, 1965)

$$\hat{n} = n\,(1 + i\kappa) \qquad (B.25)$$

where both the quantities n and κ are real. The quantity n is the ordinary refractive index and κ is the attenuation index. The quantities n and κ may be expressed in terms of the material constants ε, μ, and σ. Setting equation (B.24) equal to equation (B.25) gives the relation

$$n^2\,(1 - \kappa^2) = \mu\varepsilon \qquad and \qquad n^2\kappa = \frac{2\pi\mu\sigma}{\omega}. \qquad (B.26)$$

It is noted that experimental values of the optical constants n and κ for a variety of materials may be found, for example, in Born and Wolf (1965).

B-4

REFERENCES

Born, M., and E. Wolf. 1965. *Principles of Optics*, Pergamon Press, Oxford, England.

Morrill, W. K. 1961. *Analytic Geometry*, International Textbook Company, Scranton, PA.

APPENDIX C

ELECTROMAGNETIC BOUNDARY CONDITIONS

The electromagnetic boundary conditions that must be satisfied at the planar interface $z = z_p$ separating subregions p and $p+1$ (see figure C1 below) are contained in the matrix equation (33). This equation has been rewritten in equation (C.1) below for convenience

$$\begin{bmatrix} C_1\varepsilon & C_2 \\ C_2 & C_1\mu \end{bmatrix}_p \begin{bmatrix} f_1 \\ f_2 \end{bmatrix}_p = \begin{bmatrix} C_1\varepsilon & C_2 \\ C_2 & C_1\mu \end{bmatrix}_{p+1} \begin{bmatrix} f_1 \\ f_2 \end{bmatrix}_{p+1}. \qquad (Interface\ z = z_p) \qquad (C.1)$$

$$z = z_p$$
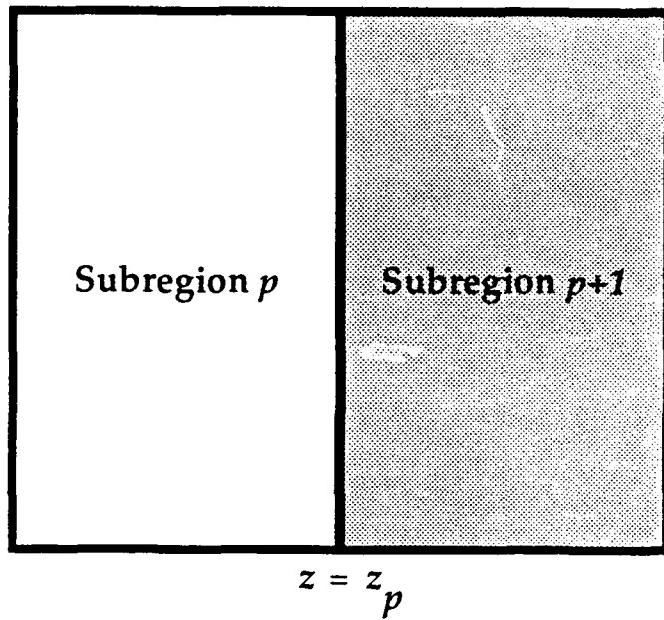
Figure C1. Planar interface $z = z_p$ separating subregions p and $p+1$.

The matrices $[C_1]$ and $[C_2]$ appearing in equation (C.1) are given by equation (30). Equation (C.1) can be written in the following simplified form

$$\begin{bmatrix} G_1 & O \\ O & G_2 \end{bmatrix}_p \begin{bmatrix} f_1 \\ f_2 \end{bmatrix}_p = \begin{bmatrix} G_1 & O \\ O & G_2 \end{bmatrix}_{p+1} \begin{bmatrix} f_1 \\ f_2 \end{bmatrix}_{p+1}. \qquad (Interface\ z = z_p) \qquad (C.2)$$

by using the following identity

$$\begin{bmatrix} C_1 & C_2 \\ C_2 & C_1 \end{bmatrix} \begin{bmatrix} C_1\varepsilon & C_2 \\ C_2 & C_1\mu \end{bmatrix} \equiv -\begin{bmatrix} G_1 & O \\ O & G_2 \end{bmatrix}. \tag{C.3}$$

The matrices $[G_1]$ and $[G_2]$ are given by

$$[G_1] = \begin{bmatrix} 1 & 0 & 0 & 0 \\ 0 & 1 & 0 & 0 \\ 0 & 0 & \varepsilon & 0 \\ 0 & 0 & 0 & \varepsilon \end{bmatrix} \quad and \quad [G_2] = \begin{bmatrix} 1 & 0 & 0 & 0 \\ 0 & 1 & 0 & 0 \\ 0 & 0 & \mu & 0 \\ 0 & 0 & 0 & \mu \end{bmatrix}. \tag{C.4}$$

It can be easily shown that the single matrix equation (C.2) is equivalent to the following four boundary conditions in vector form evaluated at $z = z_p$:

(1) The tangential component of the electric field is continuous

$$\{\hat{z} \times E\}_p = \{\hat{z} \times E\}_{p+1} \tag{C.5}$$

(2) The normal component of the electric displacement is continuous

$$\{\hat{z} \bullet D\}_p = \{\hat{z} \bullet D\}_{p+1} \tag{C.6}$$

(3) The tangential component of the magnetic field is continuous

$$\{\hat{z} \times H\}_p = \{\hat{z} \times H\}_{p+1} \tag{C.7}$$

(4) The normal component of the magnetic induction is continuous

$$\{\hat{z} \bullet B\}_p = \{\hat{z} \bullet B\}_{p+1} \tag{C.8}$$

The vectors $E, H, D,$ and B appearing in equations (C.5) through (C.8) are given by

$$E = (E_x, E_y, E_z) \quad and \quad H = (H_x, H_y, H_z) \tag{C.9}$$

$$D = \varepsilon(E_x, E_y, E_z) \quad and \quad B = \mu(H_x, H_y, H_z). \tag{C.10}$$

The unit vector $\hat{z}$ points along the positive z-direction.

We will now restrict our attention to equation (C.2) for the special case of monochromatic plane-wave solutions previously described in detail in appendix B. It is a well known fact that a dielectric multilayer optical medium illuminated by a monochromatic electromagnetic plane-wave will give rise to two monochromatic plane-waves propagating in opposite directions within each layer of the multilayer medium (Fowles, 1968). The electromagnetic field vector associated with any subregion within the multilayer medium may, therefore, be represented by the superposition of two electromagnetic field vectors

$$
\begin{bmatrix} f_1 \\ f_2 \end{bmatrix} = \begin{bmatrix} f_1 \\ f_2 \end{bmatrix}_R + \begin{bmatrix} f_1 \\ f_2 \end{bmatrix}_L .
$$

(C.11)

Each of the field vectors on the right-hand side of equation (C.11) has the monochromatic plane-wave representation given by equation (B.2) in appendix B, that is,

$$
\begin{bmatrix} f_1 \\ f_2 \end{bmatrix}_R = \begin{bmatrix} f_{01} \\ f_{02} \end{bmatrix}_R exp\{i\,[r]^T\,[k]_R\}
$$

(C.12)

$$
\begin{bmatrix} f_1 \\ f_2 \end{bmatrix}_L = \begin{bmatrix} f_{01} \\ f_{02} \end{bmatrix}_L exp\{i\,[r]^T\,[k]_L\} .
$$

(C.13)

The subscripts R and L denote wave propagation to the right and left respectively. Substitution of equation (C.11) into equation (C.2) leads to

$$
\begin{bmatrix} G_1 & O \\ O & G_2 \end{bmatrix}_p \left\{ \begin{bmatrix} f_1 \\ f_2 \end{bmatrix}_R + \begin{bmatrix} f_1 \\ f_2 \end{bmatrix}_L \right\}_p = \begin{bmatrix} G_1 & O \\ O & G_2 \end{bmatrix}_{p+1} \left\{ \begin{bmatrix} f_1 \\ f_2 \end{bmatrix}_R + \begin{bmatrix} f_1 \\ f_2 \end{bmatrix}_L \right\}_{p+1} .
$$

(C.14)

For equation (C.14) to be satisfied for all values of time, t, the angular frequencies of the individual plane-waves in the two subregions, p and $p+1$, must satisfy the equation

$$
\{\omega_R\}_p = \{\omega_L\}_p = \{\omega_R\}_{p+1} = \{\omega_L\}_{p+1} = \omega .
$$

(C.15)

Similarly, for equation (C.14) to be satisfied for all values of x and y on the planar boundary $z = z_p$, the x- and y-components of the wave vectors associated with each of

the individual plane-waves in the two subregions, p and $p+1$, must satisfy the equations

$$\{k_{xR}\}_p = \{k_{xL}\}_p = \{k_{xR}\}_{p+1} = \{k_{xL}\}_{p+1} = k_x \qquad \text{(C.16)}$$

$$\{k_{yR}\}_p = \{k_{yL}\}_p = \{k_{yR}\}_{p+1} = \{k_{yL}\}_{p+1} = k_y. \qquad \text{(C.17)}$$

From equation (B.19) it is apparent that the wavenumbers associated with the R and L waves in any subregion within the multilayer medium must be equal, namely

$$\{k_R\}_p = \{k_L\}_p = k_p \qquad and \qquad \{k_R\}_{p+1} = \{k_L\}_{p+1} = k_{p+1}. \qquad \text{(C.18)}$$

With the use of equations (C.16), (C.17), (C.18) and (B.7), (B.8) from appendix B, it can be easily shown that the z-components of the wave vectors associated with each of the individual plane-waves in the two subregions, p and $p+1$, must satisfy the equations

$$\{k_{zR}\}_p = -\{k_{zL}\}_p = \{k_z\}_p \qquad \text{(C.19)}$$

$$\{k_{zR}\}_{p+1} = -\{k_{zL}\}_{p+1} = \{k_z\}_{p+1}. \qquad \text{(C.20)}$$

With the use of equations (C.12) through (C.20), the matrix equation (C.14) takes on the finalized form

$$\begin{bmatrix} G_1 & O \\ O & G_2 \end{bmatrix}_p \left\{ \begin{bmatrix} f_{01} \\ f_{02} \end{bmatrix}_R exp\,(+iz_p k_z) + \begin{bmatrix} f_{01} \\ f_{02} \end{bmatrix}_L exp\,(-iz_p k_z) \right\}_p = \qquad \text{(C.21)}$$

$$\begin{bmatrix} G_1 & O \\ O & G_2 \end{bmatrix}_{p+1} \left\{ \begin{bmatrix} f_{01} \\ f_{02} \end{bmatrix}_R exp\,(+iz_p k_z) + \begin{bmatrix} f_{01} \\ f_{02} \end{bmatrix}_L exp\,(-iz_p k_z) \right\}_{p+1}.$$

REFERENCE

Fowles, G. R. 1968. *Introduction to Modern Optics*, Holt, Rinehart, and Winston, Inc., New York, NY.

REPORT DOCUMENTATION PAGE

1. AGENCY USE ONLY *(Leave blank)*	2. REPORT DATE October 1993	3. REPORT TYPE AND DATES COVERED Final: September 1993

4. TITLE AND SUBTITLE A NEW MATRIX FORMULATION OF CLASSICAL ELECTRODYNAMICS Part III. Wave Propagation Through A Multilayer Dielectric Medium With Planar Boundaries	5. FUNDING NUMBERS PE: 0603218C PROJ: 76-EE43 01 WU: DN303143
6. AUTHOR(S) R. P. Bocker	

7. PERFORMING ORGANIZATION NAME(S) AND ADDRESS(ES) Naval Command, Control and Ocean Surveillance Center (NCCOSC) RDT&E Division San Diego, CA 92152-5230	8. PERFORMING ORGANIZATION REPORT NUMBER TD 2569

9. SPONSORING/MONITORING AGENCY NAME(S) AND ADDRESS(ES) Office of the Chief of Naval Research (Code 4414) 800 North Quincy Street Arlington, VA 22217	10. SPONSORING/MONITORING AGENCY REPORT NUMBER

11. SUPPLEMENTARY NOTES

12a. DISTRIBUTION/AVAILABILITY STATEMENT Approved for public release; distribution is unlimited.	12b. DISTRIBUTION CODE

13. ABSTRACT *(Maximum 200 words)*

    A new approach for solving electromagnetic wave propagation problems is currently being developed at the Naval Command, Control and Ocean Surveillance Center (NCCOSC), RDT&E Division (NRaD). This new approach is based upon an 8 by 8 matrix representation of the Maxwell field equations. In addition, a computer software package based on this matrix representation of electromagnetic theory is also being written and tested at NRaD to handle a variety of scenarios involving electromagnetic wave propagation through matter. This software package is referred to as the MATURE Program. MATURE is the acronym for Matrix Approach To Understanding Relativistic Electrodynamics. The MATURE Program is written in MATLAB code for use on a Sun 4 SPARCstation 2 workstation. Under Independent Research (IR) FY 92 funding, this matrix approach was successfully employed in solving problems dealing with electromagnetic wave propagation through dielectric, crystalline, linear electro-optic, and magneto-optic materials of infinite extent. Under the Office of Naval Research (ONR) FY 93 funding, this matrix formulation was extended to handle problems involving wave propagation through multilayer dielectric media with planar boundaries. Presented in this technical document is the underlying theory of this matrix approach. Several numerical examples, based on the use of the MATURE Program, are also included to illustrate the use of the matrix approach in solving electromagnetic wave propagation problems.

14. SUBJECT TERMS electromagnetic wave propagation electric field vector matrix representation magnetic field vector dielectric medium reflectance Maxwell field equations transmittance	15. NUMBER OF PAGES 70
	16. PRICE CODE

17. SECURITY CLASSIFICATION OF REPORT UNCLASSIFIED	18. SECURITY CLASSIFICATION OF THIS PAGE UNCLASSIFIED	19. SECURITY CLASSIFICATION OF ABSTRACT UNCLASSIFIED	20. LIMITATION OF ABSTRACT SAME AS REPORT

Standard form 298 (FRONT)

21a. NAME OF RESPONSIBLE INDIVIDUAL	21b TELEPHONE (include Area Code)	21c OFFICE SYMBOL
Dr. Richard P. Bocker	(619) 553-6404	Code 761